PROBE BEAM DEFLECTION: A NOVEL IN-SITU ELECTROCHEMICAL TECHNIQUE

Barbero, C.A.; Miras, M.C.

Departamento de Química, Universidad Nacional de Río Cuarto,
Agencia postal No 3, 5800-Río Cuarto, ARGENTINA
TE & FAX: +54 358 4676 233. E-mail: cbarbero@exa.unrc.edu.ar

Abstract

The basic aspects of Probe Beam Deflection techniques, used to detect concentration gradients in electrochemical systems, are described. The theory of the different techniques is first discussed. Then, a critical review of published applications of the techniques to various electrochemical systems is performed. Among the systems whom these techniques has been applied are: electrochromic oxides, conducting polymers, redox polymers, underpotential deposition, surface electrochemical reaction on solid electrodes, oscillatory phenomena, double layer charging and metal deposition.

Resumen

Los aspectos básicos de las técnicas de Deflectometría por Gradiente de Concentración (Probe Beam Deflection), que se usan para detectar gradientes de concentración en sistemas electroquímicos, son descriptos. Inicialmente se discute la teoría de las diferentes técnicas. Posteriormente, se realiza una revisión crítica de los resultados publicados acerca de la aplicaciones de las técnicas a diversos sistemas electroquímicos es realizada. Entre los sistemas a los cuales estas técnicas han sido aplicadas están: óxidos electrocrómicos, polímeros conductores, polímeros redox, deposición a subpotenciales, reacciones superficiales en electrodos sólidos, fenómenos oscilatorios, cargado de doble capa y deposición de metales.

1. Introduction

Electrochemistry deals with the interaction of electricity with chemical systems. Classic electrochemical studies were based on the study of electron fluxes trough the electrode solution interface [1] While using different perturbation techniques and/or changes of the electrolyte media (e.g. pH), it has been possible to give information about electrochemical mechanisms, it become obvious that purely electrochemical techniques have significant limitations. Therefore, a plethora of in-situ techniques has been developed in recent years, where spectroscopic techniques have been combined with electrochemical perturbations to help to understand electrochemical phenomena. Most of those techniques have been applied to study the electrode/solution interface [2]. On the other hand, the study of fluxes in solution, coupled to the electrochemical reactions has been more limited. While electron flux is often determined by the mass transport in solution, there are few techniques able to study the concentration gradients coupled to

electrochemical reactions. One of these techniques is interferometry. It has relatively low sensitivity, slow response and both complex experimental set-up and analysis. Therefore it was used mainly to the study of metal electrodeposition in electroplating cells and similar systems [3]. More recently, some other techniques have been used to detect ion fluxes in solution like radioactivity [4], pH sensors [5], fluorescence or absorption measurement on grid electrodes [6], scanning electrochemical microscopy [7], and ring-disk voltammetry [8]. Even more related to the present subject, McCreery and co-workers performed diffraction spectroelectrochemistry in the visible optical region [9] and Kragt et al [10] used an interferometric microscope to measure concentration gradients in front of an electrode.

A new technique, which is able to measure concentration gradients in a fast and simple manner, has been recently developed. Spectroscopist used a technique which is based on the detection of thermal gradients which are formed by optical absorption, followed by non radiative decay (Photothermal Deflection Spectroscopy, PDS [11-13]) Specifically, in PDS the thermal gradients are detected trough the coupled refractive index gradients using a laser beam which suffers refraction. During the application of PDS to electrochemical systems, it was found that the probe beam suffers a significant deviation in absence of light. It was reasoned that electrochemical reactions could also produce refractive index gradients due to gradients of concentration of of reactants/products [11]. Therefore, using the signals in absence of radiation, a technique usually called "Probe Beam Deflection (PBD)", was developed. The technique has also been known as "Mirage Effect" (while the name "Mirage effect" predates the other names, given the physical phenomena it evoques, it seems more appropriate to leave such name for thermal and not concentration techniques) or, less commonly, "Optical Beam Deflection".

While in principle simple light sources (e.g. lamps) and position detectors (e.g. pinhole photodiodes) could be used to detect the deflection of the beams, it was the availability of affordable lasers and position detectors which makes the technique development possible

The mechanism of detection in PBD involves deflection (refraction) of the probe beam by the refractive index gradient. If a refractive index gradient is present in transparent medium, different parts of a beam traveling perpendicular to the gradient would traverse zones of different refractive index. The speed of light would be different for each part of the beam. Therefore, the beam will deviate. Using a small angle approximation, the deviation would obey eqn.1 [14]

$$\theta(x,t) = \left(\frac{l}{n} \frac{\partial n}{\partial C} \right) \left(\frac{\partial C(x,t)}{\partial x} \right) \qquad [1]$$

Where C is the concentration, l is the interaction path length, n is the refractive index of the bulk and dn/dC is the variation of refractive index with concentration. The possible perturbations used in PBD are as diverse as those used in electrochemistry. Therefore, the basic principles will be initially stated, then details for each experimental technique will be described, and finally the actual application to electrochemical systems will be discussed.

1.1 Basics

The deflection of a probe beam, which travels close to an electrode along a path length *l,* in an electrolyte of refractive index *n* (Figure 1) could be understood as a distortion in the wave front of the beam. The wave speed increases according to $v = c/n$. In conditions of small deflection, the geometric optics approximation could be used. Therefore, the relationship between refractive index and concentration gradients obey eqn. 1. To obtain the equations governing the PBD signal for different electrochemical techniques, the formula for the concentration gradient has to be obtained. A given electrochemical system could be modeled as a flat electrode of width *w* in contact with a semi-infinite fluid layer where diffusion occurs (being the diffusion layer several times thinner than *w*). The latter condition imply that border effects could be neglected and the interaction path length *l = w*. Using the mass transport equations and the boundary conditions, the variation of concentration gradient with time and distance could be obtained. Since electrochemical reactions occur in the electrode surface (x = 0), the diffusion of a specie in the diffusion layer obey eqn. [2]

$$\frac{\partial^2 C}{\partial x^2} = \frac{1}{D}\frac{\partial C}{\partial t} \qquad [2]$$

with the boundary conditions; $C(x,0) = C_o$ for all x and $\lim_{x \to \infty} C(x,t) = C_o$ for all t.
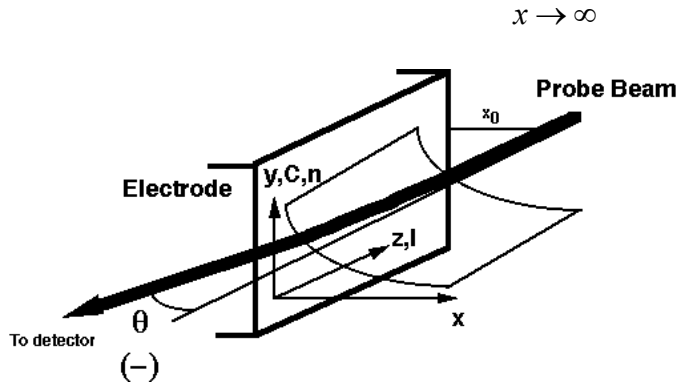

Figure 1: Probe Beam Deflection. Scheme of the deflection phenomena

Once the concentration gradient $\dfrac{\partial C(x,t)}{\partial x}$ is calculated, the deflection can be obtained from eqn. 1.

In electrochemistry, the concentration gradient is usually calculated at the electrode surface (x = 0) because, in that way, the mass transport is directly related with the electron flux (current) trough Faraday equation (3):

$$i = n_e FA\left[\frac{\partial C(x,t)}{\partial x}\right]_{x=0} \qquad [3]$$

Nevertheless, in PBD it is necessary to simulate the flux at a finite distance (x) where the centre of the probe beam is. In principle a laser beam could be focused in a point, as small as the wavelength (632.8 nm for an He-Ne laser) However, the path length would be also of the size of the wavelength. Applying eqn. 1, the signal would be small. For finite path lengths (e.g. 1 cm), the beam cannot be focused below a waist (given by Gaussian optics) of ca. 60 mm. Therefore the centre of the beam would be at ca. 30 mm away from the electrode surface. Since the probe beam centre is at a finite distance of the electrode (typically 30-180 mm), the PBD signal is delayed in time with respect to the current signal due to diffusion of the ions. Such delay is the time that take the concentration perturbation to travel between x = 0, where is produced, and the beam centre, where is monitored.

In general, to obtain the equations to simulate the PBD response, the following steps have to be carried out:

1) Obtain the concentration profile at distance x $C(x,t)$ for the system under study.

2) Differentiate with respect to x, to obtain $\dfrac{\partial C(x,t)}{\partial x}$.
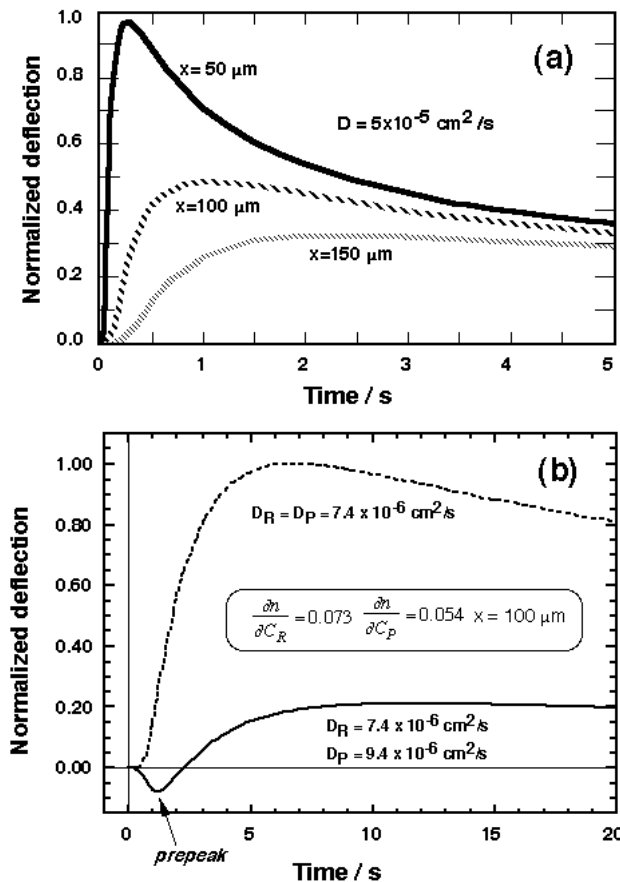
3) Combine with eqn. 1 to obtain $\theta(x,t)$

Figure 2: *Simulated Potential Pulse Chronodeflectometry plots during a continuous process. (a) Effect of beam-electrode distance. (b) Both reactant and product soluble, effect of different diffusion coefficient.*

1.2 Techniques
1.2.1 Potential Step Chronodeflectometry

This technique consists in applying a potential pulse to the system, from a potential where there is no reaction to one where the reaction is complete, and monitor the time evolution of the PBD signal. It is of simple mathematic treatment. Therefore, more different variants of the technique have been explored than with any other PBD technique.

1.2.1.1 Continuous process with binary electrolyte

Those electrochemical systems where a soluble substance is continuously produced, consumed or transformed are called continuous processes. If a binary electrolyte is present (only two species, e.g. HCl) the migration and diffusion are coupled trough the electroneutrality condition. That is, the species cannot move faster than a arithmetic median of the diffusion coefficient of anions and cations.

Solving the mass transport equations gives the concentration equation[1]

$$C(x,t) = C_0 \, erf\left(\frac{x}{\sqrt{4Dt}}\right) \tag{4}$$

Where C is the concentration, x is the beam-electrode distance, t is the time and D is the diffusion coefficient of the binary electrolyte. The concentration gradient is obtained as the derivative with respect to the distance x:

$$\frac{\partial C(x,t)}{\partial x} = \frac{C_o}{\sqrt{\pi Dt}} e^{-x^2/4Dt} \tag{5}$$

The formula for the PBD signal is obtained combining [5] and [1]:

$$\theta(x,t) = \left(\frac{l}{n}\frac{\partial n}{\partial C}\right)\frac{C_o}{\sqrt{\pi Dt}} e^{-x^2/4Dt} \tag{6}$$

Simulated chronodeflectometry profiles obtained using eqn. 6 are shown in Figure 2.a. As it can seen, the signal shows a maxima at a given time, which depends on the distance. Finding the maxima by differentiation of eqn. 1 with respect to time, renders:

$$\sqrt{t_{max}} = \frac{(x - x_0)}{\sqrt{2D}} \tag{7}$$

Using eqn. 7, the diffusion coefficients (D), of binary electrolytes, could be measured by chonodeflectometry [15]. To do that, chronodeflectometric profiles are obtained while the beam-electrode distance is changed from an initial value x_0. Additionally, the initial beam-electrode distance could be obtained.

The value of PBD signal at the maxima only depends on Co and x: (eqn. 8)

$$\theta_{max}(x) = \left(\frac{l}{n}\frac{\partial n}{\partial C}\right)\frac{C_o}{x} * 0.484 \tag{8}$$

Equations 6 and 7 are only valid for systems where only one substance is generated or consumed (e.g. metal deposition). If a substance is converted into another

by a redox change (e.g. $Fe(CN)_6^{-4}$ into $Fe(CN)_6^{-3}$ by oxidation), the contribution of both components have to be taken into account, and a more complex formula is obtained:

$$\theta(x,t) = \left(\frac{l}{n}\right)\left\{\left[\left(\frac{\partial n}{\partial C_R}\right)\frac{C_o}{\sqrt{\pi D_R t}}e^{-x^2/4D_R t}\right] - \left[\left(\frac{\partial n}{\partial C_P}\right)\frac{C_o\left(D_R/D_P\right)}{\sqrt{\pi D_P t}}e^{-x^2/4D_P t}\right]\right\} \quad [9]$$

Where R and P means reactant and product respectively. Then, the shape of the chronodeflectometric profile would depend on the relative values of the diffusion coefficients (D_R and D_P) and refractive index gradients (dn/dC_R and dn/dC_P).

For some values of R and P diffusion coefficients (such as those of the $Fe(CN)_6^{-4}$ / $Fe(CN)_6^{-3}$ couple), even prepeaks of opposite sign could be observed (Figure 2.b, full line). If we assume that $D_R=D_P$ (Figure 2.b, upper broken line), a common assumption in electrochemistry, eqn. 9 reduces to:

$$\theta(x,t) = \left(\frac{l}{n}\right)\left(\frac{\partial n}{\partial C_R} - \frac{\partial n}{\partial C_P}\right)\frac{C_o}{\sqrt{\pi D t}}e^{-x^2/4D t} \quad [10]$$

It has been shown that, theoretically, for species with different $\partial n/\partial C$ it is possible to simulate different profiles including null deflection or inverted sign (decrease of deflection during conversion) [16]. Therefore, it is important to know the values of $\partial n/\partial C$ before performing an experiment. Those values could be obtained, for stable species, measuring the refractive index of solutions with different concentrations. In Table 2 (Appendix) are depicted the values of $\partial n/\partial C$ reported in the literature.

It is noteworthy that $\partial n/\partial C$ values of liquids and solids are positive, while the corresponding values for gases are negative. Additionally, it can be seen that $\partial n/\partial C$ values could vary up to 2 orders of magnitude. Therefore it could be possible detect concentration changes of one species with a big $\partial n/\partial C$ in presence of another with smaller coefficients, even if the concentration of the later changes more significantly.

The complexities of PBD response in redox systems make the technique of little use when redox transformation of solution species is considered. As it will be seen, the forte of the technique is to study exchange of ions by solid state (redox oxides, metals, conductive polymers, etc.) species.

1.2.1.2 Continuous processes with no binary electrolyte

This is a more general case where more than two ionic species are present. Especially relevant is the case, common in electrochemistry, where an inert salt is added to maintain high ionic conductivity (and low migration of the electroactive substance), the so called "supporting electrolyte". Vorotyntsev et al [17] solved the complete Nernst-Planck equation (diffusion + migration) for a solution containing an electroactive species (M) and a supporting electrolyte (KA), where one of the inert salt ions (K^+ or A^-) is the counterion of the electroactive species.

The expression for the PBD signal is then (11):

$$\theta(x,t) = G_{op}\left\{\left[\left(\frac{\partial n}{\partial C_M}\right)_K + z\left(a - \frac{1}{2}\right)\left(\frac{\partial n}{\partial C_K}\right)_M\right]\left(e^{-x^2/4D_M t}\right) - za\left(\frac{\partial n}{\partial C_K}\right)_M\left(e^{-x^2/4D_{KA} t}\right)\right\} \quad [11]$$

with $G_{op} = \left(\dfrac{l_e}{n}\right)\left(\dfrac{c_o}{\sqrt{\pi D_M\, t}}\right)$ and $a = 0.25(D_K^{-1} - D_A^{-1})(D_{KA}^{-1} - D_M^{-1})^{-1}$

Equation 11 simplifies to eqn. 10 when the species M is neutral or $(\partial n/\partial C_K)_M$ is negligible. In fact, NH$_4$OH, has a very low $(\partial n/\partial C_K)_M$ (0.00091). Therefore, it has been used as supporting electrolyte in PBD measurements of soluble species [18]. It is important to note that the use of non binary electrolyte is only necessary if the diffusion coefficient of the electroactive species is to be estimated, or the necessary conditions (pH, ionic strength) could not be achieved with binary electrolytes. As a rule, use of non binary electrolytes for PBD measurements should be avoided.
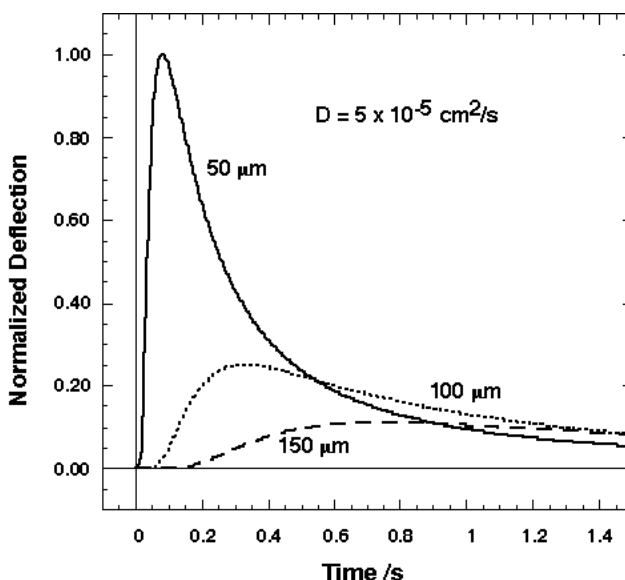

Figure 3: *Cronodeflectometry during discontinuous process. Effect of beam-electrode distance.*

1.2.1.3 Instantaneous or discontinuous processes

In this kind of systems, the amount of species produced or consumed is finite. Examples are the electrodisolution of a thin layer (less than 10 monolayers) metal deposit, ion exchange occurring when a film of a solid electroactive substance (redox oxide, conductive polymer, electroactive polymer, etc.) is oxidised or reduced, the charging/discharging of a double layer and the metal ions produced when an amalgam is stripped of its metal content.

If the rate of reactions inside the layer have to be taken into account, it is necessary to know the kinetics of the process and its study is possible with PBD. However, a simplified case of general use could be solved easily. To do that, it is

assumed that production/consumption of all species occurs in a time span negligible with respect to time width of the PBD pulse. Therefore the concentration profile at the initial time corresponds to a Dirac delta function. The approximation is valid for thin electroactive films with a thickness of several monolayers. However, it is important to remember that the switching time has to be negligible relative to the time of the measurement. As we will see below, measuring with beam-electrode distances higher than the minimum allows applying the approximation to systems switching in seconds.

Using the assumption, the Fick law is solved for semi-infinite linear diffusion, giving the dependence of concentration with time and distance:

$$C(x,t) = \frac{C_S}{\sqrt{\pi Dt}} e^{-x^2/4Dt} \qquad [12]$$

Where Cs is the total concentration of ions exchanged in the process. Differentiation with respect to x, and combining with eqn.[1] gives the expression for deflection as:

$$\theta(x,t) = \left(\frac{l}{n}\frac{\partial n}{\partial C}\right)\frac{C_s}{\sqrt{\pi Dt}}\frac{x}{2Dt}e^{-x^2/4Dt} \qquad [13]$$

The plot of PBD as a function of time (Figure 3) presents maxima as in the continuous process which decays faster. As in the former case, it is possible to estimate the time of the maxima, as a function of the beam-electrode distance:

$$\sqrt{t_{max}} = \frac{(x - x_0)}{\sqrt{6D}} \qquad [14]$$

The equation could be used to estimate diffusion coefficients (D) and x_0 from chronodeflectometric data. In the simplest case, there is only one species moving. This is true only for binary electrolyte. Again, the value of PBD at the maxima only depends on C_S and x:

$$\theta_{max}(x) = \left(\frac{l}{n}\frac{\partial n}{\partial C}\right)\frac{C_S}{x^2} * 0.925 \qquad [15]$$

Since metal deposition and re-dissolution can be studied by PBD, the reduction of Ag^+ to metal and the layer re-dissolution was used to check the validity of chonodeflectometric equations. The chronodeflectometric profile during deposition obeys a continuous process (Figure 4.a), while the re-dissolution of the thin layer obeys discontinuous process (Figure 4.b). Using the dependence of the time of the maxima on the beam-electrode distance, for both processes, a value of $D_{Ag^+} = 1.5 \times 10^{-5}$ cm^2/s, was measured. The value agrees well with those reported in literature [19].

A similar behaviour was observed for the ion exchange of an electroactive polymer film (poly(o-phenilenediamine)) [20] and the ion exchange of an electrochromic oxide film [19], suggesting that the equations for a discontinuous process could successfully be applied to those systems.
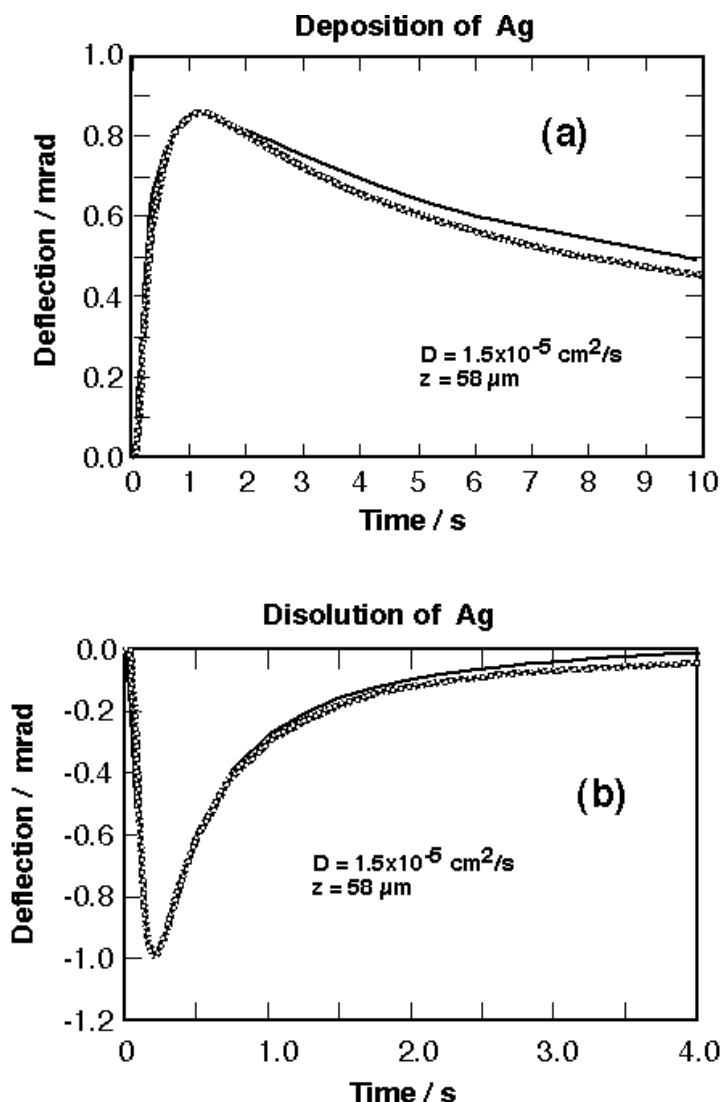
Figure 4: *Cronodeflectometry of silver. Solution = 1.5 mM AgClO$_4$ in 2 M HClO$_4$. D = 1.5x10^{-5} cm^2/s. x= 58 mm. (a) Deposition of Ag. Initial Potential = 0.9 Vsce. Final Potential = 0.3 Vsce. Gray line = experimental data. Black line = simulated with eqn. 13. (b) Dissolution of Ag. Initial potential = 0.3 Vsce. Final potential = 0.9 Vsce. Gray line = experimental data. Black line = simulated with eqn. 16.*

1.2.2 Pulse Deflectometry

The chonodeflectometry has the advantage, over other PBD techniques such as cyclic deflectometry, to have a closed analytical form for the equations describing the process. However, it only allows studying the changes between two extreme states (e.g. redox states in a polymer). To be able to study the dependence of the ion fluxes with the applied potential, the general dependence of PBD with potential has to be obtained. If we apply potential pulse between a fixed potential and different potentials, the concentrations gradients will depend on time and potential. Each plot has a profile

similar to the one found for chronodeflectometry but the intensity depends on E. In Figure 5.a, the dependence of $C_S(E)$ with E was assumed to follow Nernst equation. If the amount of ions exchanged ($C_S(E)$) at x = 0 does not depend upon time, the general expression of PBD could be obtained:

$$\theta(E,t) = U(t)\left(\frac{l}{n}\frac{\partial n}{\partial C}\right)C_{ion}(E) \qquad [16]$$

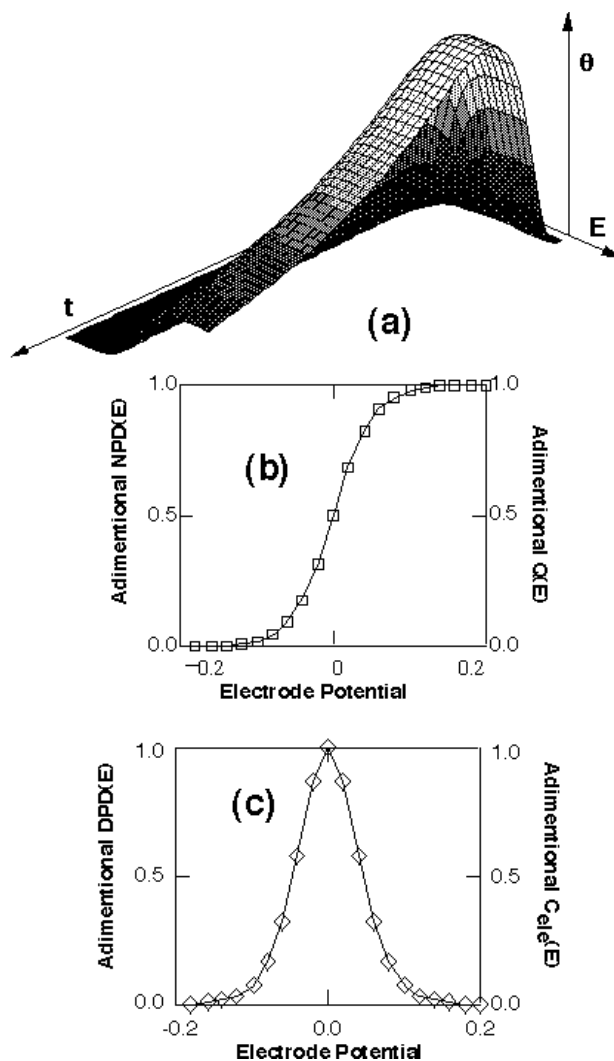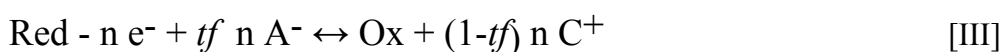Where the factor U(t) contains all temporal parameters (eqn. 6 or 13) which are independent of E.

Figure 5: *Simulated curves for Pulse Deflectometry. (a) Tridimensional plot of PBD as a function of time and potential for a reversible continuous process. (b) Comparison of NPD(E) (points) with charge (line) for the process described in (a). (c) Comparison of the DPD(E) signal (points) with the current (line) for the process described in (a)*

The value of deflection could be obtained at any point of the PBD chonodeflectometric curve. However, the maximum value (at t = t_{max}) would have the best signal/noise ratio. In that case U(t) reduces to a factor dependent on x (eqn.8 or 15).

The dependence of PBD on E at t=t_{max} measures effectively the concentration of exchanged species at each potential. It could be called Normal Pulse Deflectometry (NPD(E)) (Figure 5.b), in analogy to the Normal Pulse Voltammetry. Its derivative with respect to the applied potential could be similarly called Differential Pulse Deflectometry (DPD(E)) (Figure 5.c).

Surface Redox process

In the case of redox coupled ion exchange in electroactive films, the charge compensation could occurs via anions, cations or both. This is described in the equations:

$$\text{Red - n e}^- + \text{n A}^- \leftrightarrow \text{Ox} \tag{I}$$

$$\text{Red - n e}^- \leftrightarrow \text{Ox} + \text{n C}^+ \tag{II}$$

$$\text{Red - n e}^- + tf \text{ n A}^- \leftrightarrow \text{Ox} + (1-tf) \text{ n C}^+ \tag{III}$$

For cases [I] and [II], the NPD(E) signal obeys eqn. 15 :

$$NPD(E) = \theta(E)_{t=t_{max}} = U(t_{max})\left(\frac{\partial n}{\partial C}\frac{l}{n}\right)t_f\left(\frac{Q(E)}{n_e F}\right) \tag{17}$$

Where tf is the transference number, which is +1 [I] or -1 for [II], n_e is the number of electrons exchanged by each redox center, Q(E) is the charge and F is the Faraday constant. As the charge is also related with n_e, a straight line of unitary slope between NPD(E) and Q(E) imply only one ion used to balance charge.

In case [III], the equation describing the process is:

$$NPD(E) = \theta(E)_{t=t_{max}} = U(t_{max})\left(\frac{\partial n}{\partial C}\frac{l}{n}\right)\left[2t_f(E)-1\right]\left(\frac{Q(E)}{n_e F}\right) \tag{18}$$

If the plot of NPD(E) vs. Q(E) is not a straight line, it is possible to detect potential ranges where a simple ion flux exists and to obtain the transference number ($ft(E)$.) for each ion. If it is a straight line, the slope could be different to unity, indicating that a mixed exchange exists an a common $tf(E)$ value could be calculated using eqn.17.

Similarly, the Differential Pulse Deflectometry (DPD(E)) represents a capacity of ion movement and is related with the electric capacitance and the voltammetric current by:

$$DPD(E) = U(t_{max})\frac{\partial C_s(E)}{\partial E} = \frac{t_f}{n_e F}\frac{\partial Q}{\partial E} = \frac{t_f}{n_e F}C_{ele} = \frac{t_f}{n_e F}\frac{i(E)}{v} \tag{19}$$

Where C_{ele} is the electrical capacitance in farads, tf is the ion transference number and v is the potential scan rate of the cyclic voltammogram (it is assumed thin layer conditions for the electroactive layer, in practice a small enough scan rate) mesured in the same experience.

Equations 18 and 19 are equivalent, but it would be simpler to compare the cyclic voltammogram (normalised with v) with the DPD(E) profile. This could be done by numerical differentiation of NPD(E). However, such procedure decreases the signal/noise ratio. An alternative procedure to obtain DPDE(E) imply experimentally measuring the PBD signal during pulses with a fixed potential step and shifting initial potentials. The difference between PBD signal at each state is in fact DPD(E).

From eqn. 18, it is possible to obtain the dependence of NPD(E) (and DPD(E)) with the potential for any known dependence of $C_S(E)$ with E. In the case of Nernst equation, the deflection would be:

$$NPD(E) = \theta(E)_{t=t_{max}} = U(t_{max})\left(\frac{l}{n}\frac{\partial n}{\partial C}\right)C_{ion}\left(\frac{e^{-\frac{nF}{RT}(E-Eo)}}{1+e^{-\frac{nF}{RT}(E-Eo)}}\right) \qquad [20]$$

In that way, the reversibility or ideality of a given system could be evaluated from PBD measurements. Similar equations could be obtained for other known $(Cs(E))$ dependences (e.g. Butler/Volmer equation).
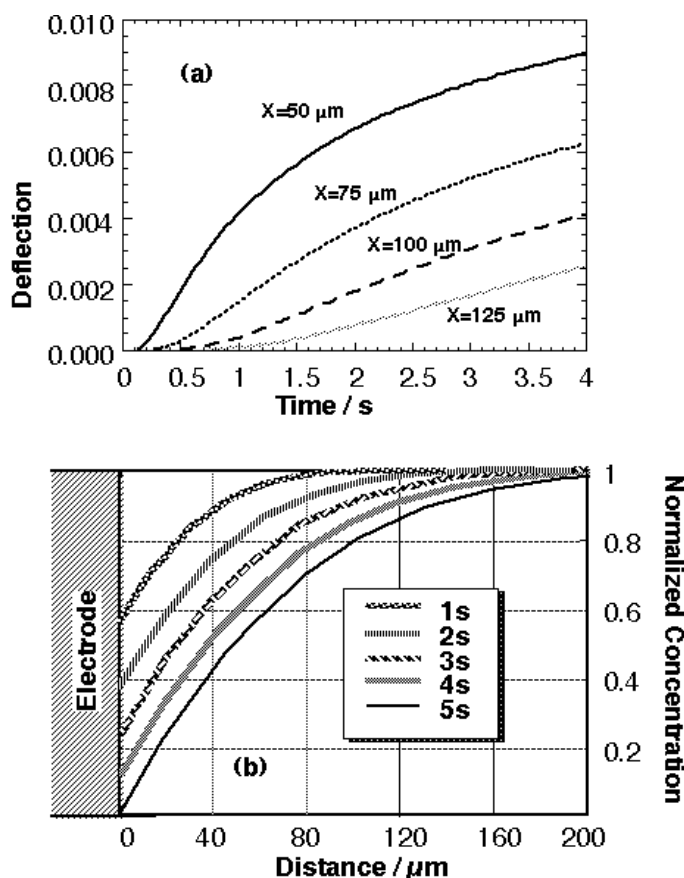

Figure 6: *Simulated curves for current pulse chronodeflectometry. Do= 1 x 10^{-5} cm^2/s. j=1 A. $\partial n / \partial C$ = 0.02. (a) Effect of the beam-electrode distance (eqn. 22). (b) Concentration (calculated using eqn. 23) as a function of distance for fixed times.*

1.2.3 Current Step Cronodeflectometry

Another possible perturbation is a current pulse. The theory was developed by Decker and co-workers [21]. Passing trough the cell a current density (j) at t =0, the mass flux in x = 0 is fixed (eqn. 3). The concentration profile will be:

$$C(x,t) = \frac{j}{n_e FD} \left[2\sqrt{\frac{Dt}{\pi}} e^{\left(x^2/4Dt\right)} - x \; erfc\left(\frac{x}{\sqrt{4Dt}}\right) \right] \qquad [21]$$

where j is the current density and n_e is the number of electrons exchanged. Differentiating with respect to x and combining with [1] gives the expression for PBD signal at constant current.

$$\theta(x,t) = \left(\frac{l}{n}\frac{\partial n}{\partial C}\right) \left[\frac{j}{n_e FD} erfc\left(\frac{x}{\sqrt{4Dt}}\right) \right] \qquad [22]$$

In Figure 6 are shown the profiles at different beam-electrode distances. It is also possible to know the concentration profile as a function of distance, at constant time. In that way the behavior of technologically interesting systems, such as battery electrodes or metal deposition cells, could be investigated. Since such an study has been extensively made by interferometry [22], it is worthy to compare the capability of PBD in that field. By integration of curve described by eqn. 22, the concentration profile is obtained from PBD (eqn. 23):

$$Co(x) = \left(\frac{l}{n}\frac{\partial n}{\partial C}\right)^{-1} \int_o^x \theta(x)dx \qquad [23]$$

In Figure 6.b it is shown the expected concentration profiles as function of the distance. To calculate it experimentally, it is necessary to measure the PBD signal while the beam-electrode distance is varied. This can be done by scanning the beam, using the refraction in a moving glass slab [23] or moving the cell, using a driver, while the beam is kept stationary [24]. In the later study, using the galvanostatic deposition of Cu, eqn. 23 was fitted for small current densities and the onset of convective processes at long times detected (Figure 7).

1.2.4 Alternating Current Deflectometry

Another perturbation is a sinusoidal current of potential. Decker and co-workers [25] developed the theory for alternating current. When an alternating current density ($j = j_o sin\omega t$) is applied to the electrode, the concentration on the electrode surface, applying Fick law for semi-infinite diffusion on a flat electrode, will be:

$$C(x,t) = C_0 + \left(\frac{j_0}{n_e F\sqrt{Dw}}\right) exp\left(-\sqrt{\frac{\omega}{2D}}x\right) sin\left(\omega t - \sqrt{\frac{\omega}{2D}} - \frac{\pi}{4}\right) \qquad [24]$$

where w is the angular frequency of the sinusoidal perturbation. Differentiation with respect to x, and combining with eqn. 1, gives the expression for PBD signal:

$$\theta(x,t) = -\left(\frac{l}{n}\frac{\partial n}{\partial C}\right)\left(\frac{j_0}{n_e F\sqrt{Dw}}\right)\sqrt{\frac{\omega}{2D}}\exp\left(-\sqrt{\frac{\omega}{2D}}x\right)sin\left(\omega t - \sqrt{\frac{\omega}{2D}} - \frac{\pi}{4}\right) \quad [25]$$

The amplitude of the signal is proportional to the perturbation amplitude (j_O) according to:

$$\left|\theta(x,w)\right| = -\left(\frac{l}{n}\frac{\partial n}{\partial C}\right)\left(\frac{j_0}{n_e F\sqrt{Dw}}\right)\sqrt{\frac{\omega}{2D}}\exp\left(-\sqrt{\frac{\omega}{2D}}x\right) \quad [26]$$

The logarithm of amplitude and phase are lineal with the beam-electrode distance (x), with slope $p = -\sqrt{\omega/2D}$. From that slope, diffusion coefficients have been evaluated [26].
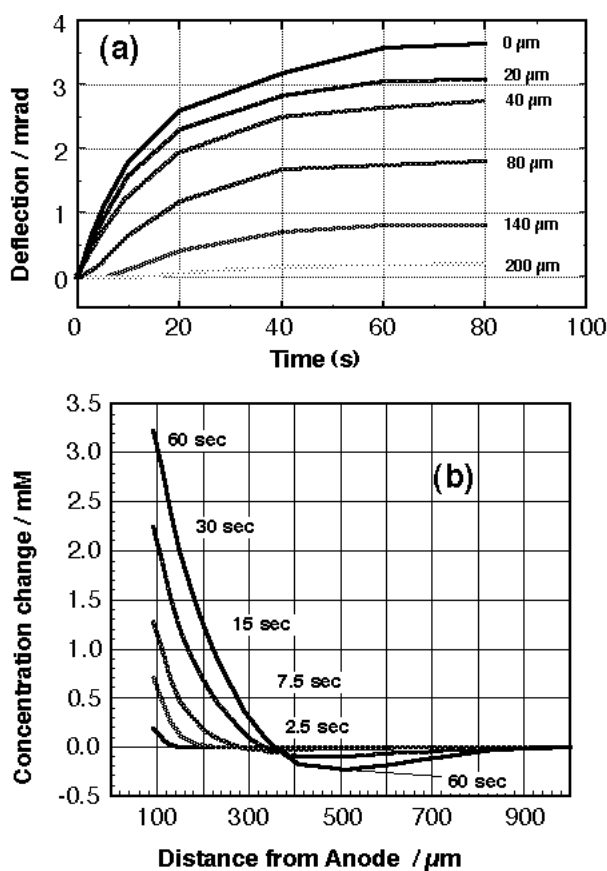

Figure 7: *Current during Cu deposition at constant current.[CuSO$_4$] = 0.1 M. (a) Current chronodeflectometry at different distances. (b) Concentration profiles at different times.*

1.2.6 Cyclic VoltaDeflectometry

Unlike the previous cases, it is not possible to obtain an analytical expression for the relationship between PBD signal and potential when the potential is scanned linearly ($E = E_{inicial} + vt$) at a constant scan rate ($v = \partial E/\partial t$). Therefore, cyclic

voltadeflectometry experiments, where the PBD signal is monitored along the cyclic voltamperogram, could not be analytically simulated. A similar situation exists with cyclic voltamperometry, where a closed form does not exists [1]

An additional problem of voltadeflectometry resides in the diffusional delay (see 1.1). This appears as a potential difference between the peak in voltadeflectometry and the corresponding peak in voltamperometry. In simple systems that delay does not interfere with the analysis. However, in some systems it is observed a null PBD signal in a potential range where the current is not zero. This could be due to null ion flux (equal fluxes of opposite magnitude) or caused by the delay. To be able to compare current and PBD, the delay has to be eliminated. One possible way to do that involves measuring at very low scan rates, to minimize the potential delay. However, the magnitude of PBD signal, as any diffusionally controlled flux, is proportional to the square root of the scan rate. Therefore, at low scan rates the signal/noise ratio will deteriorate.

In an analogue fashion to voltammetry, two methods could be used to overcome the problem: a) digital numeric simulation and b) convolution of the experimental signal. Both methods could be used to simulate the PBD signal (at a beam-electrode distance x) or to transform the experimental signal into a flux in the electrode surface (at x=0), to be compared with the current signal.

1.2.6.1 Digital numeric simulation

This is the more general approach but is more complex to be carried out. Mathias [26] used it to simulate the ion exchange in poly(1-hydroxyphenazine) in a binary electrolyte ($HClO_4$). The flux at x=0 was calculated from the PBD data and the diffusion coefficients of the species. The calculation method used was orthogonal collocation. Rudnicki et al [16] used a similar approach, but they calculate the PBD signal from a given flux at x=0 and use the simulation to evaluate the effect of the diameter of the beam and other experimental parameters. It was found [16] that a beam of diameter inferior 100 μm can be considered thin for the deflection, that is the measured deflection is equivalent to that one measured for a point beam.

1.2.6.2 Convolution technique

The convolution technique is well known in electrochemistry and was developed independently by Saveant and coworkers [27] and Oldham and co-workers [28]. The technique was applied to evaluate concentrations at a distance from the electrode by Engstrom and co-workers [29] and Oldham and co-workers [30]. The technique was applied to process PBD data by Pawliszyn [31] and developed further by Vieil and co-workers [32].

To apply the method to cyclic voltadeflectometry, the following assumptions are made:

i) that electron flux is directly linked to ion flux
ii) that electron exchange and ion exchange occurs simultaneously.
iii) that all ion exchange occurs in a time period significantly lower than the time that takes the gradient to reach the electrode. This one is, in fact, the definition of a discontinuous or instantaneous process.

The measured electronic current, i(t), is equal to the sum of ionic fluxes in the electrode-solution interface:

$$i(t) = FA\sum z_k J_k(0,t) \qquad [27]$$

where there is a contribution k for each ion exchanged and $J_k(0,t)$ represents the flux of each species at x = 0. Each mole of substance exchanged carries a charge $z_k F$. To evaluate the flux of each ion at a distance and time ($J_k(x,t)$), the convolution product of a mass transfer function is applied to the flux in the electrode surface.

$$J_k(x,t) = H(x,t) * J_k(0,t) \qquad [28]$$

Where * indicates the convolution product. For a mass transport (in a binary electrolyte) from/to an electrode with semi-infinite diffusion, the solution of Fick law gives a mass transfer function:

$$H(x,t) = \frac{x}{2\sqrt{(\pi D t^3)}} e^{-x^2/4Dt} \qquad [29]$$

Applying eqn.28 and combining with eqn. 1 renders:

$$\theta(x,t) = \left(\frac{l_e}{n}\frac{\partial n}{\partial C}\right)\left(\frac{1}{D_{MA}}\right)\left[\left(\frac{x}{2\sqrt{(\pi D_{MA}t^3)}} e^{-x^2/4D_{MA}t}\right) * i(t)\right] \qquad [30]$$

The procedure was validated using the silver deposition/stripping as in the case of chronodeflectometry by Hillman and co-workers [33]. It is noteworthy that applying eqn. 28 to the concentration profile at t =0, x =0 in the case of potential pulses would render eqn. 6 (for the continuous case) and eqn. 13 (for the discontinuous case). However, in that case it is better to apply the analytical solution than numerical convolution since the concentration profiles for pulse potential presents a singularity that makes the numerical procedures unstable. In fact, the procedure has to be applied to the chronocoulometric profile to avoid mathematical unstability [34].

Vieil et al perform a quantitative analysis, using convolution techniques, of the redox coupled ion exchange between poly(phenylene) films and a binary electrolyte [35], the profiles were then simulated [36]. Vieil and Lopez [37] have compared the redox coupled ion exchange in polypyrrole with that in poly(pyrrolesulfonate). The flux of co-ions, together with counterions, was detected trough the comparison of the ion flux at x=0 with the current.

A parameter necessary to apply the procedure is the diffusion coefficient of the species exchanged. In a binary electrolyte, only one diffusion coefficient exists (D_{MA}). One strategy to do that, consists in measuring the voltadeflectogram at different distances and to compare it with the PBD signal simulated with eqn. 30. Using literature values for $\partial n/\partial C$, the value of $x/\sqrt{D_{MA}}$ which fits the experimental data is evaluated. Another strategy implies measuring the chronodeflectometric profiles at different distances and to obtain the D_0 and x_0 from eqn.14.

If a good fitting of the convoluted signal with currents is obtained, the ion exchange model (kind and number of ions) represents the system. Otherwise, some potential ranges where a different ion flux is present could be detected. An experimental drawback of the convolution method is that the potential window for voltadeflectometry is smaller than the one for voltamperometry, due to the potential delay. Since the extreme potentials are defined by other constraints, such as electrode or electrolyte stability, some information could be lost.
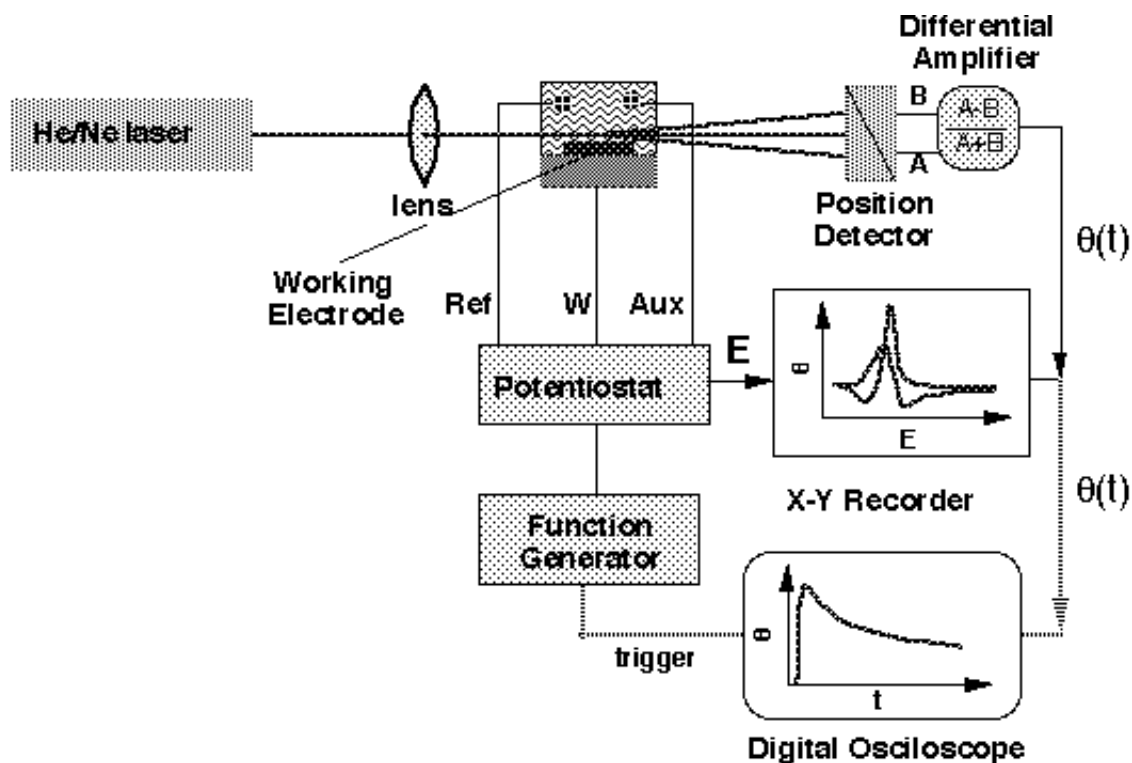

Figure 8: *Experimental set-up for Probe Beam Deflection.*

1.3 Experimental set-up

In Figure 8 is shown a scheme of a typical PBD set-up, which is similar to the one described before [38]. The basic components of the PBD system are a 5 mW He-Ne laser (Melles Griot, 05 LHP11) and a bicell position sensitive detector (UDT PIN SPOT /2D). The laser beam is focused by a 50 mm lens to a diameter of roughly 60 mm in front of the planar electrode. The electrochemical cell, an optical glass cuvette with 2 cm of path length, is mounted on a 3 axis tilt table (Newport). A micrometric translation stage allows for controlled positioning of the sample with respect to the laser beam in 10 mm steps. The position sensitive detector is placed 25 cm behind the electrochemical cell and has a sensitivity of 3 mV/ 1 mm, which resulted in a deflection sensitivity of 1 mrad/V. All parts of the system are mounted on an optical rail and the set-up is mounted on an optic table (Melles Griot). The deflection signal is processed using a position monitor (UDT 201 DIV). Due to the fact that slow signals have to be monitored, the whole

system is warmed up for 24 Hs before each measurement to eliminate thermal fluctuations. All optical equipment is asembled on an optical table.

The signals of the two photodiodes, in the bicell detector, are subtracted and normalised to the overall signal to eliminate laser intensity fluctuations. A digital oscilloscope (HP 5462), for fast measurements, or a multimeter (HP 3428), for slow measurements, connected trough IEEE488 port to a personal computer are used for monitoring the PBD signal during potential step experiments. A XY recorder (Linseis LY 14100-11) is used for recording the PBD signal along with the cyclic voltammogram. The working electrodes can be any flat solids such as polished glassy carbon plates, Pt plates, Au films on glass, ITO/glass transparent electrodes, carbon aerogel plates, etc.

1.4 Applications of Probe Beam Deflection in Electrochemistry.

Subsequently, we describe the application of PBD techniques to different electrochemical phenomena.

1.4.1 Solution species
1.4.1.1 Ferrocyanide/Ferricyanide

As it has been discussed, the study of redox systems in solutions is difficult due to inherent complexity of the concentration profiles. However, soluble redox systems have been used to test the techniques. The cyclodeflectometric signal observed during oxidation of ferrocyanide shows a peak with a potential shift (due to the time delay) with respect to the peak in voltamperometry [16]. The chonodeflectometry presents a positive peak with a small pre peak. The response seems to be due to the sum of the ferrocyanide and ferricyanide PBD profiles. Being the dn/dC higher for ferrocyanide than for ferricyanide (Table 2), the first dominates the overall PBD signal. The pre peak is caused by the difference of diffusion coefficients, for $Fe(CN)_6^{-3}$ (Do = 9.4 10^{-6} cm^2/s) and $Fe(CN)_6^{-4}$ (Do = 7.4 10^{-6} cm^2/s). The minor contributor to the PBD signal is faster and dominates at short times.

1.4.1.2 Oxygen reduction

A more interesting system is the reduction of oxygen. The reduction of oxygen on Au in basic media (0.1 M KOH) was studied by PBD [39]. In the voltammetric curve, two waves are observed corresponding to:

$$O_2 + H_2O \xrightarrow{+2e^-} HO_2^- + OH^- \qquad\qquad [IV]$$

$$HO_2^- + H_2O \xrightarrow{+2e^-} 3\ OH^- \qquad\qquad [V]$$

The deflection would depend on the concentration gradients of O_2, HO_2^- and OH^-. In the experimental data, a single wave at ca. +0.4 V is observed. Taking into account the $\partial n/\partial C$ values (KOH = 0.0097, H_2O_2 = 0.0014 and O_2 = -0.014), it is apparent that the later will dominate the signal, and then only O_2 reduction is observed. As it can be seen, the study of soluble species is of complex interpretation.

1.4.1.3 Oscillatory phenomena

While oscillatory phenomena are quite complex in their own, PBD could be used to evaluate the role of solution species in the oscillations. On case of electrochemical oscillatory phenomena is the galvanostatic oxidation of formic acid [40]. The system was studied using PBD [41]. A clear correlation of the potential oscillations with deflection oscillations, was observed (Figure 9), suggesting a role of solution species in the oscillations. To clarify the issue, the oxidation of formic acid is studied using PBD. During the oxidation (E > 0.45 Vsce), a positive deflection is observed. Such flux could be assigned to CO_2 generation (CO_2, as a gas, has a negative $\partial n / \partial C$). It seems that the electrode initially becomes poisoned, and then the potential increases and the poison is oxidized, allowing the potential to decrease. During the oxidation of the poison, CO_2 is not produced, as the PBD decreases. In a similar fashion, PBD techniques have also been used to study the oscillatory phenomena present during corrosion of Si in HF[42].
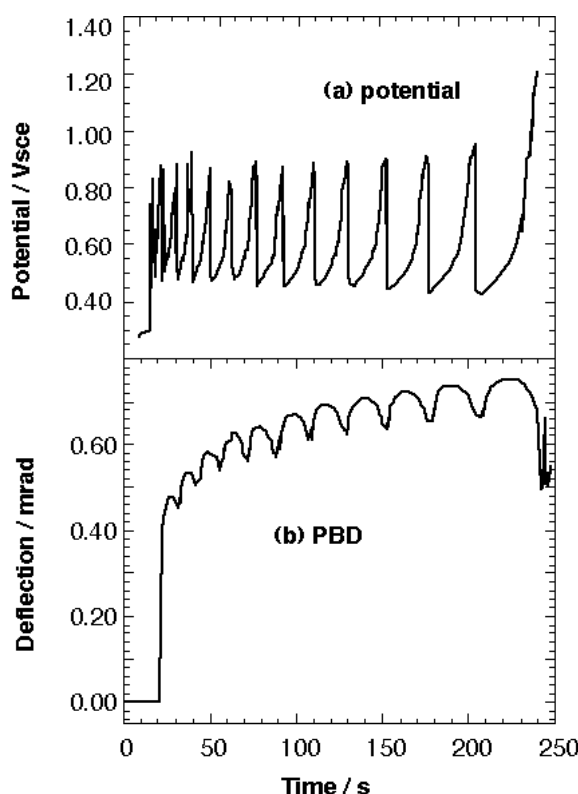

Figure 9: *Plot of the potential (a) and deflection (b) during the potential oscillation for the galvanostatic oxidation of formic acid. j = 2 mA/cm^2. [HCOOH] = 5. [HClO$_4$] = 1 M.*

1.4.1.4 Metal deposition and corrosion

Cairns and co-workers studied the oxidation of Cu in basic media using PBD and Photothermal Deflection Spectroscopy (PDS) [43]. Eriksson studied the concentration profiles in a Cu deposition cell [44]. PBD has also been used to study electroless deposition of nickel [45]. The insertion/expulsion of hydrogen in Pd electrodes at open

circuit conditions was elucidated by PBD [46]. The etching of Si in basic [47] and acidic fluoride [48] was also monitored by PBD.

1.4.2 Surface systems
1.4.2.1 Oxide monolayers

One of the electrochemical systems most thoroughly studied is the cyclic voltammogram of polycrystalline Pt in aqueous media. This system was initially studied by Rudnicki et al [12], using multiple cycles and averaging to improve the signal/noise ratio. Then, it was studied by Kersetz et al [41] using single cycle but with an electrode of increased area (> 11 times), trough platinization.

The cyclic voltammogram and the corresponding PBD signal are observed in Figure 10. During oxidation, the concentration of protons increases (positive deflection) due to the oxidation of adsorbed hydrogen, followed by a region with negligible signal in the double layer region and a clear increase of concentration (negative deflection) coming from the metal reaction with water to form the oxide:
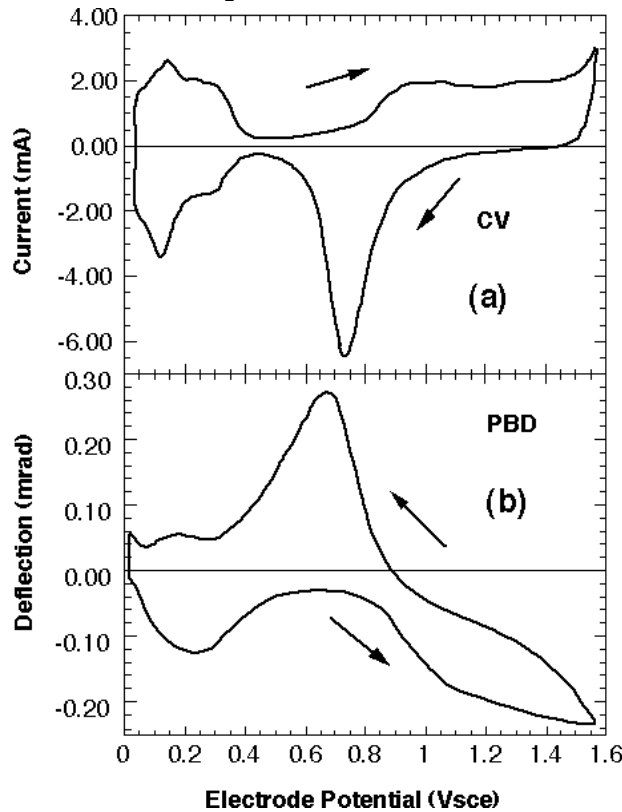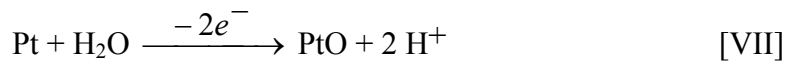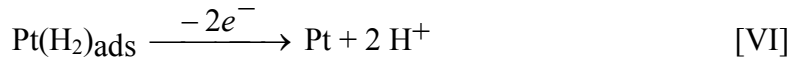
$$Pt(H_2)_{ads} \xrightarrow{\ -2e^-\ } Pt + 2\,H^+ \qquad\qquad [VI]$$

$$Pt + H_2O \xrightarrow{\ -2e^-\ } PtO + 2\,H^+ \qquad\qquad [VII]$$


Figure 10: *Cyclic voltamperogramm (a) and voltadeflectogramm (b) for a polycrystalline Pt electrode in 1 M HClO$_4$. v= 100 mV/s. Rugosity of ca. 17.*

During reduction, the opposite reactions occur, with the opposite PBD signal observed. The system has been then studied by Cairns and co-workers [49]. They observed similar behavior in acid and basic media. They also show a qualitative effect of the anions in the double layer regions, being able to detect the double layer charging and to detect the potential dependent ion adsorption of ClO_4^-, $H_2PO_4^-$ and Cl^-.

A similar behavior is observed with gold electrodes [39]. In this metal, hydrogen adsorption is minimal. Only the signal due to oxide formation is detected:

$$Au + H_2O \xrightarrow{\;-2e^-\;} AuO + 2\,H^+ \qquad\qquad \text{[VIII]}$$
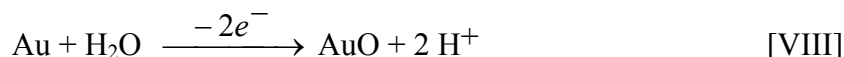
In such system, the adsorption of anions in the double layer region could be easily detected. The PBD signal switch sides at the potential of zero charge (E= -0.2 Vsce). Another electrode material, glassy carbon, was also studied by PBD [39]. In this case, the polished electrode has a weak current and PBD signal. However, after electrochemical activation (oxidation at 2.0 Vsce in acid media), clear current and PBD signal are observed. During oxidation, proton concentration decreases (negative deflection), with the opposite signal during reduction. The surface reaction is assigned to be:

$$QH_2 \xrightarrow{\;-2e^-\;} Q + 2\,H^+ \qquad\qquad \text{[IX]}$$
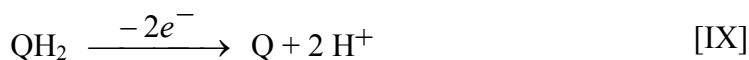
Where Q and QH_2 are the quinone and hydroquinone surface groups. The fluxes observed in polished electrodes are in the same direction, suggesting that the polished surface is covered by a native oxide layer. PBD has been also used to study the intercalation of anions in graphite [50] and in thin films of fullerenes [51]. In the later system, each redox peak is correlated with cation insertion in the film.

1.4.2.2 Under Potential Deposition (UPD)

A related system is the deposition and stripping at potentials more anodic than the reduction standard potential of metal ions. The UPD of copper on Pt was studied using PBD [39]. As it can be seen in Figure 11, it is possible to detect the different forms of metals adsorption (shown as peaks in CV and CVD). By comparison, CVD is more sensitive than CV, being able to detect 2% of a monolayer. It is likely that the higher value of $\partial n/\partial C$ for $CuSO_4$ than for H_2SO_4 (Table 2) to be responsible for such increased sensitivity.

1.4.2.3 Double layer charging/discharging

As it was described (1.4.2.1), the double layer charging of metal electrodes has been qualitatively studied using PBD. A quantitative evaluation of ion adsorption/desorption is difficult due to the small signals. A way to overcome that involves the use of electrodes with high ratio of electrochemical active area to geometric area (high rugosity). As the PBD signal measures all fluxes produced outside an interface, it integrates the contribution of the whole electrode surface. An interesting system is constituted by the high surface area carbon electrodes used in supercapacitors [52]. Using Pulse deflectometry in its normal or differential version (see above), it is possible to measure the potential of minimum charge of the material [53]. In Figure 12 are shown the pulses (Figure 12.a) and NPD(E) plots for an aerogel electrode in NaF

solution (Figure 12.b). The potential of minimum charge obtained from pulse deflectometry agrees closely with the minima of the low frequency capacitance, which represents the double layer charging inside the pores. A similar agreement is obtained in a nonaqueous electrolyte (LiClO$_4$/ACN) [53].
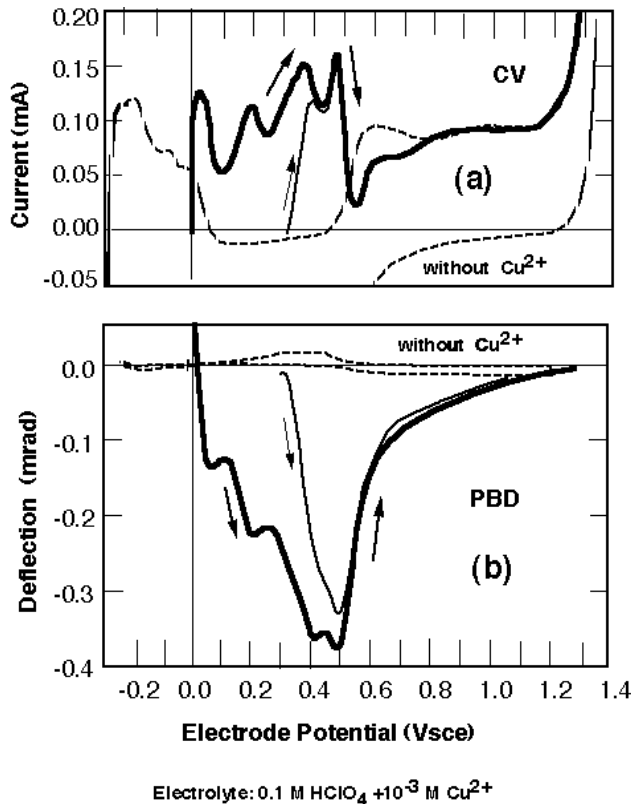

Electrolyte: 0.1 M HClO$_4$ +10^{-3} M Cu^{2+}

Figure 11: Cyclic Voltamperogramm (a) and voltadeflectogramm (b) for a Pt electrode in 0.1 M HClO$_4$. v = 100 mV/s. The broken lines represent the measurement in absemce of Cu^{2+} while the full lines show the measurement in presence of 10^{-3}M Cu^{2+}.

1.4.3 Layered systems
1.4.3.1 Electrochomic oxides

The coloration/bleaching process in electrochromic oxides involves oxidoreduction of the oxide film. Therefore, an insertion/expulsion of ions is necessary to maintain charge electroneutrality inside the oxide layer. PBD could then be used to study the ion exchange.

WO3: thin films of WO3 were produced by electrochemical oxidation of tungsten in acid media. The electrochemical response during oxidation (bleaching) is coupled with a positive deflection (ion expulsion) [38]. The flux could be explained by the reaction:
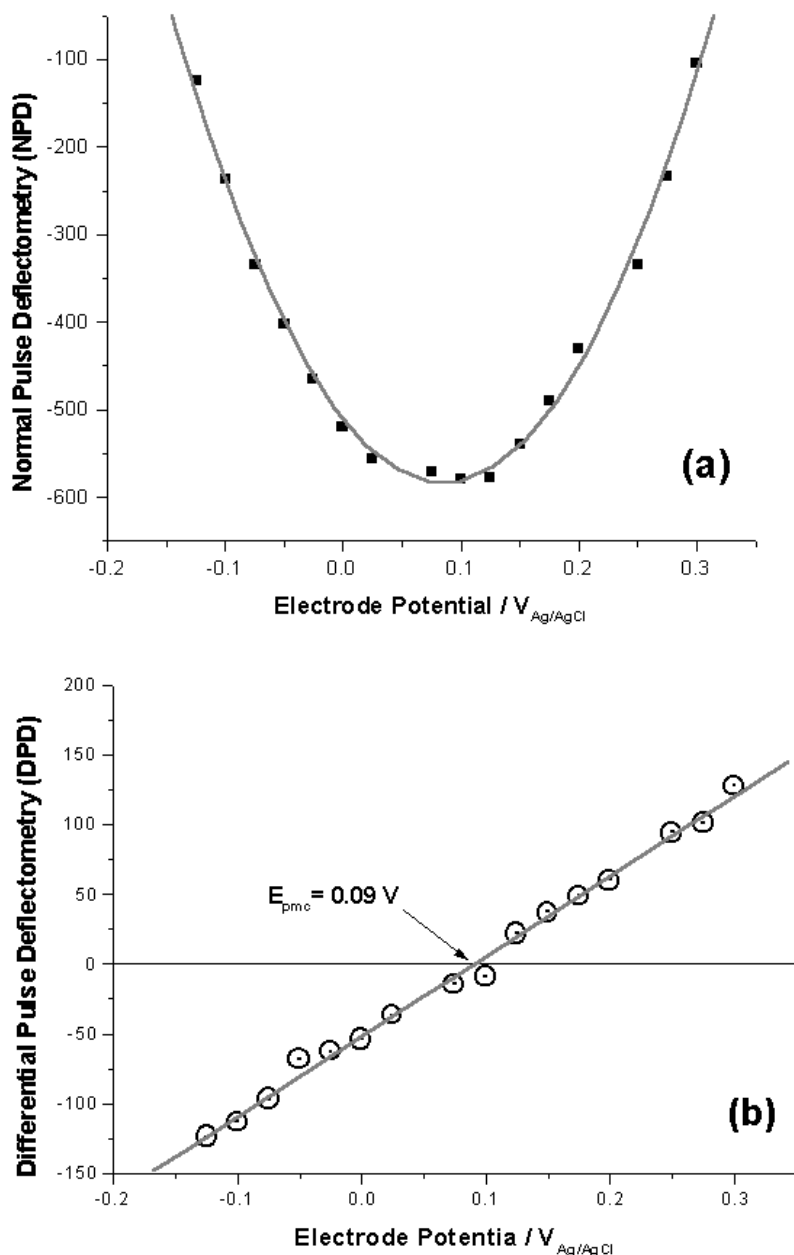
$$WO_3 \xrightarrow{\ +\ xe^-\ } WO_3H_x(H_2O)_z + x\,H^+ + z\,H_2O \qquad [X]$$
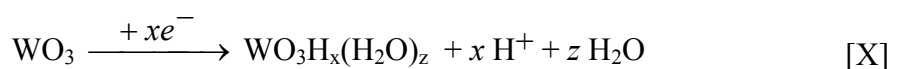
Figure 12: *Pulse deflectometry of high surface area carbon (aerogel) electrodes in 0.1 M NaF/H₂O solution. (a) Normal pulse deflectometry. (b) Differential Pulse deflectometry.*

AIROF: thin films of anodic Iridium oxide (AIROF) were synthesized by electrochemical oxidation of iridium plates [38] in acid media. In the same media (1 M $HClO_4$), the oxidation (coloration) is accompanied by negative deflection, indicating proton expulsion, like in WO_3. In basic media (1 M NaOH) the coloration is

accompanied by ion insertion (Figure 13), suggesting that the ion flux corresponds to OH⁻ insertion.

The chonodeflectometric measurements, could be fitted by eqn. 13. Using the relationship between the beam-electrode distance and the time of the maxima (eqn. 14), a diffusion coefficient of $1.7 \ 10^{-5} \ cm^2/s$ is measured in basic media and of $3.8 \ 10^{-5} \ cm^2/s$ in acid. These values agree closely with those calculated for binary electrolytes (NaOH and HClO$_4$ respectively [19]). If a supporting electrolyte is added the diffusion coefficients are $5.8 \ 10^{-5} \ cm^2/s$ and y $9.3 \ 10^{-5} \ cm^2/s$ in basic and acid media respectively. These D values agree with those of OH⁻ and H⁺ respectively [19].
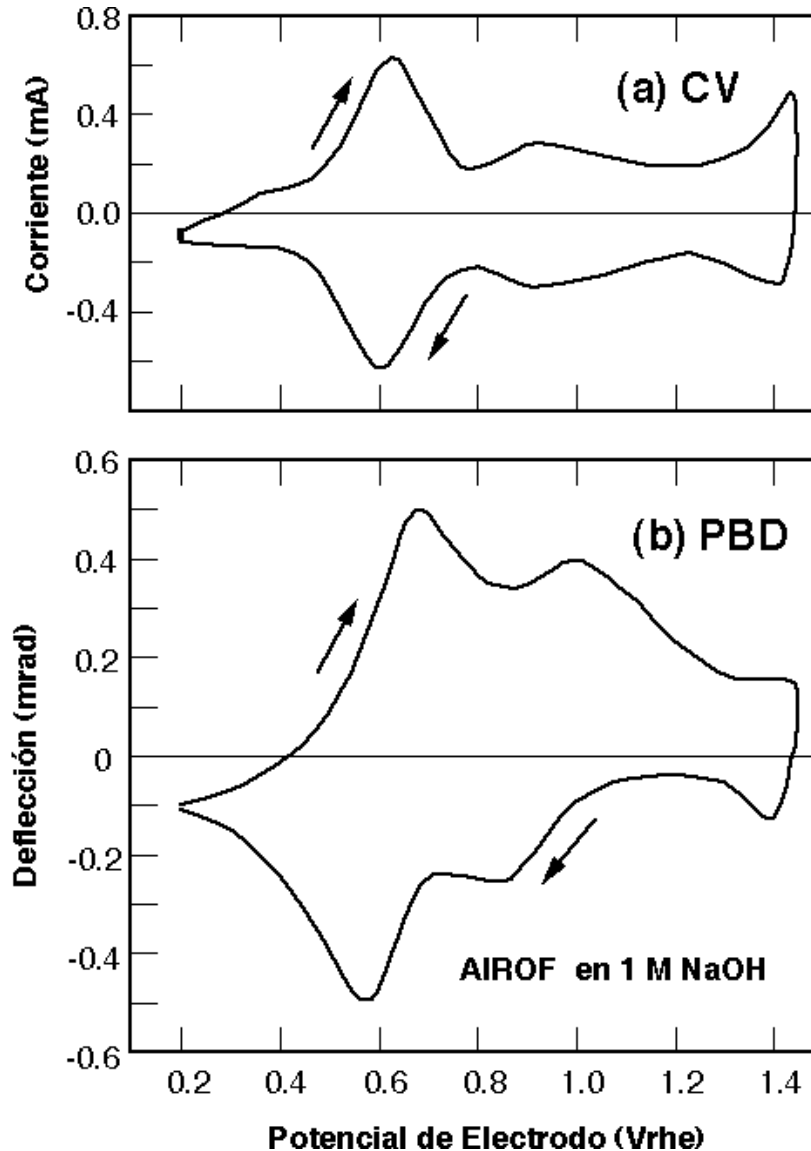

Figure 13: *Cyclic voltamperogramm (a) and voltadeflectogramm (b) for an electrode of anodic iridium oxide (AIROF) in 1 M NaOH. v= 50 mV/s.*
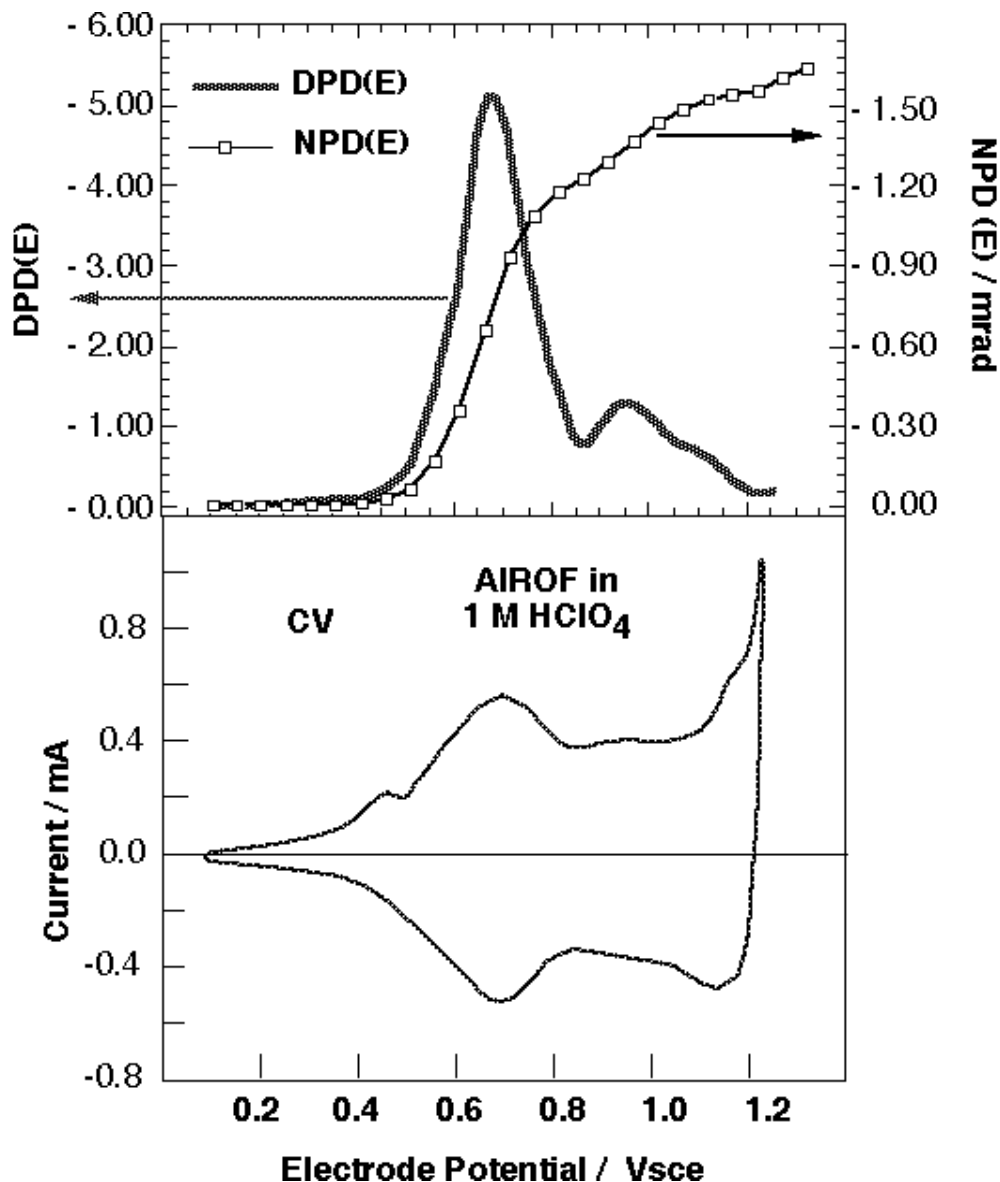
Figure 14: *Normal and Differential Pulse Deflectometry of AIROF in 1 M HClO₄. (a) Cyclic voltamperogramm. (b) NPD = points and full line. DPD = gray line.*

As it was discussed before (1.2.2), using pulse deflectometry, it is possible to compare the voltammetric and deflectometric responses without diffusional delay. The DPD(E) peaks tracks the CV (Figure 14). However, the relative intensity of the peaks is different in DPD and CV, suggesting a different ion transference number for each peak.

Those results allow proposing a mechanism of redox coupled ion exchange:

$$Ir(OH)_n \xrightarrow{-xe^-} IrO_x(OH)_{n-x} + H^+ \qquad pH<2 \qquad\qquad [XI]$$

$$Ir(OH)_n + x\ OH^- \xrightarrow{\ -x\ e^-\ } Ir(OH)_{n-x} \qquad pH<12 \qquad [XII]$$
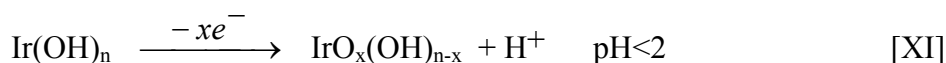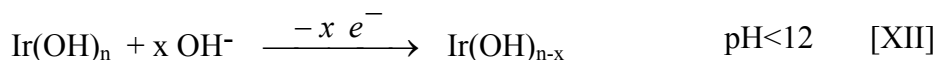
The apparent switching point for the kind of ion exchanged is between pH 3 and 4. Since the measurements between pH 3 and 11 are made using buffer solutions, the value is less certain. However, the fact that the ion exchange changes at a pH different than 7 implies that a surface property, e.g. pK_b, is measured and not the trivial predominance of the ion in higher concentration. The ion exchange of iridium oxide films deposited by evaporation was also studied [54], showing a similar mechanism.

1.4.3.2 Other oxides:

Using current pulse deflectiometry techniques, the contribution of OH^- in nickel oxide films [55], was found to be dominant with a contribution of co-ions (cations). By combination of PBD with EQCM, the role of ions and solvent was demonstrated [56].

The ion exchange in cobalt oxides was found to be mainly HO^- [1]. The chronodeflectometric response (Figure 15.a) could be simulated with the theoretical profile of a discontinuous process. The square root of the time for the maxima depends on the beam-electrode distance according to eqn. 14 (Figure 15.b), and the binary difussion coefficient for KOH was obtained. The technique has also been used to study the ion exchange ruthenium oxides [58].

1.4.3.4 Inorganic complex films

PBD techniques has also been used to study the redox coupled ion exchange in mixed salts (Ferric Ferrocyanide (Prussian blue) [59], Cupric Ferrocyanide [60], Indium Ferrocyanide [61], Luthetium diphtalocyanine [62].

1.4.3.5 Electroactive polymer films

This is the area where most extensive use has been made of PBD techniques. The first on e to be studied was the ion exchange in polythiophene [63]. Then, Haas et al studied the ionic exchange in Ru(bpi)$_2$Clpoli(4-vinylpiridine), polyaniline and poly(1-hydroxyphenazine) [64]. We will describe several studied reported in the literature, ordered from simple to more complex systems.

Poly(vinylferrocene)

This system, which has been extensively studied by other techniques (EQCM, radiotracers, etc.), was recently investigated by PBD [65]. It Thin films, deposited from a solution in toluene, were studied in aqueous and non aqueous media. In nonaqueous media (LiClO$_4$/ACN), only negative deflection accompanies oxidation. The ion exchange mechanism is the expected:

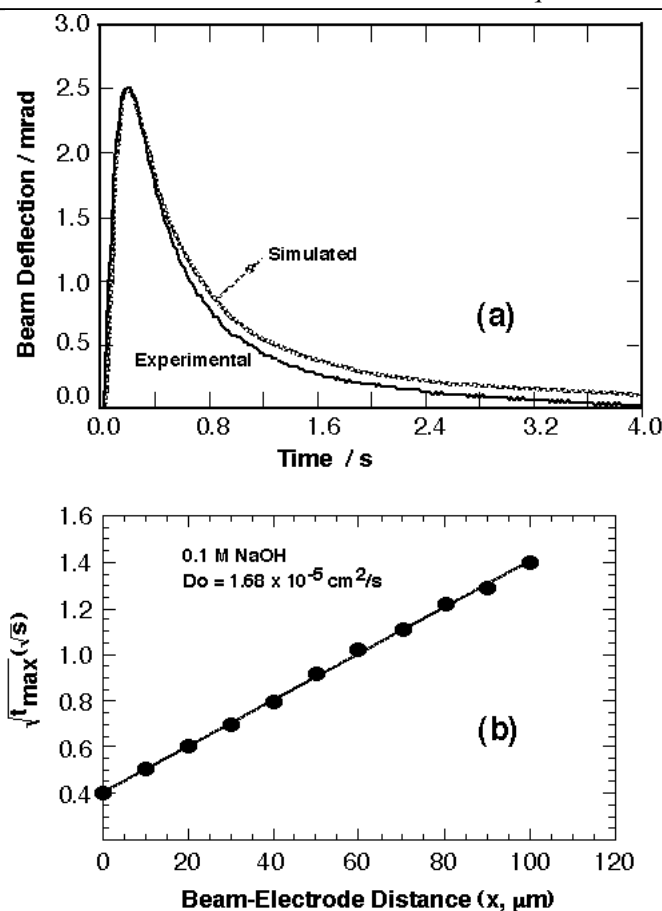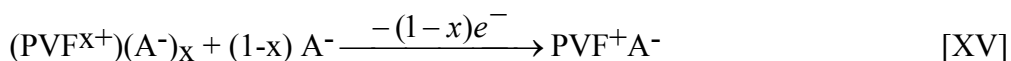$$PVF \xrightarrow{\ -e^-\ +ClO_4^-\ } PVF^+(ClO_4^-) \qquad [XIII]$$

Figure 15: *(a) Chronodeflectogram of a cobalt oxide film deposited onto a glassy carbon substrate. Solution = 0.1 M KOH. Full line is experimental data and gray line was simulated (eqn. 13) with Do = 1.7 x 10⁻⁵ cm²/s and x = 75 μm. (b) Plot of the time of the maxima in the chonodeflectograms as a function of the beam-electrode distance to calculate the diffussion coefficient of the mobile species (eqn. 14).*

In aqueous media (0.1 M $HClO_4$), a more complex mechanism is observed (Figure 16). On oxidation, a negative deflection (ion expulsion) prepeak is followed by a broad positive (ion insertion) deflection peak. Therefore, the ion exchange mechanism involves two steps:

$$PVF\ (H^+)(A^-) \xrightarrow{\ -xe^-\ } (PVF^{x+})(A^-)_X + xH^+ \qquad [XIV]$$

$$(PVF^{x+})(A^-)_X + (1-x)\ A^- \xrightarrow{\ -(1-x)e^-\ } PVF^+A^- \qquad [XV]$$

If the same system is studied in HBF_4, only negative deflection (ion expulsion) is found during oxidation (Figure 17). The results with different electrolyte acids are summarized in Table 1.
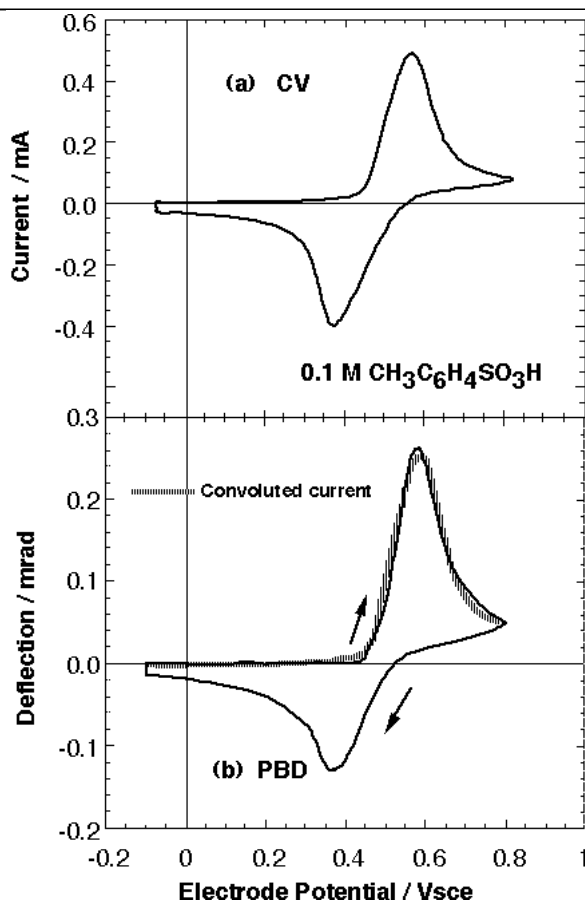
Figure 16: *Cyclic Voltamperogramm (a) and voltadeflectogramm (b) of a poly(vinylferrocene) film on GC in 0.1 M CH₃C₆H₄SO₃H/H₂O. v = 50 mV/s. The broken line in (b) was calculated using the convolution technique, with x_0= 58 μm and Do = 2.8 x 10^{-5} cm²/s.*

In Table 1 are also reported the values for the interaction coefficient between redox centres (Φ), obtained from the width of the voltammetric peak. It can be seen that negative values of Φ (repulsive interaction) corresponds to anions exchange, while positive values of Φ (attractive interaction) corresponds to cation exchange.

Polypyrrole

A clear effect of the size of the anion on the ion exchange was found in polypirrole (PPy) [66]. In HCl, polymer oxidation is followed by positive deflection (ion insertion), according to the reaction:

$$PPy^0 \xrightarrow{\ -e^- \ +Cl^- \ } (PPy^+)(Cl^-) \qquad\qquad [XVI]$$

If the solution only contains bigger anions, toluenesulfonate, a negative deflection was found, according to the mechanism:

$$PPy^0(TsO^-)(Na^+) \xrightarrow{\quad -e^- -Na^+ \quad} (PPy^+)(TsO^-) \qquad [XVII]$$
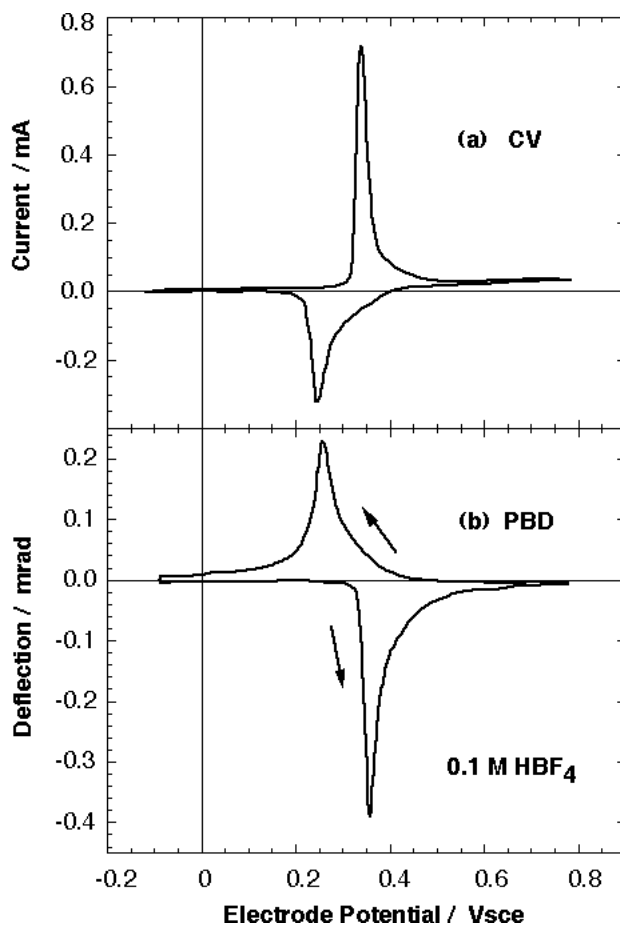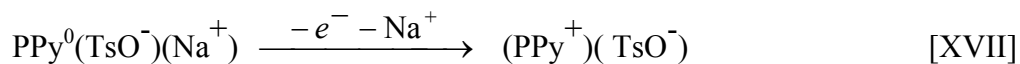
Figure 17: *Cyclic Voltamperogramm (a) and voltadeflectogramm (b) of a poly(vinylferrocene) film on GC in 0.1 M HBF₄/H₂O. v = 50 mV/s.*

Table 1. *Effect of solution electrolyte on the ion exchange mechanism and redox center interactions.*

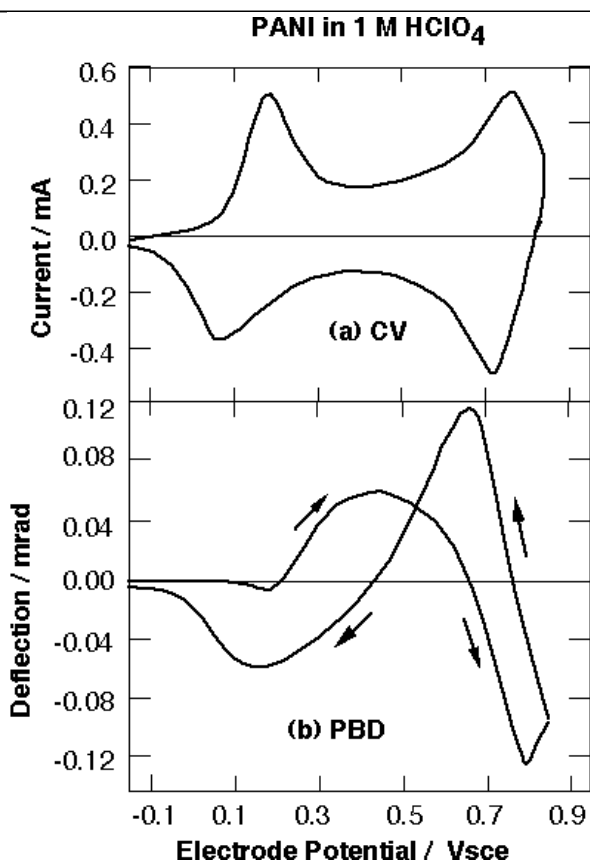| Counterion	Species exchanged	FWHM [V]	Interaction coefficient [f/M^{-1}]
$CH_3C_6H_4SO_3^-$	Anion	0.160	-0.25
ClO_4^-	Anion + Cation	0.150	-0.21
$CF_3SO_3^-$	Anion + Cation	0.100	-0.026
BF_4^-	Cation	0.080	0.046
PF_6^-	Cation	0.075	0.064

PANI in 1 M HClO$_4$

Figure 18: *Cyclic Voltamperogramm (a) and voltadeflectogramm (b) of a polyaniline (PANI) film on GC in 1 M HClO$_4$/H$_2$O. v = 50 mV/s.*

A similar case occurs when dodecylsulfate is used as counterion. Further studies using PBD confirm the trend and identify the role of the co-ions (cations) in the exchange [67-69]. In phosphate buffer solutions, PPy prepared with dihydroxybenzene disulfonate anions, also exchange cations [70].

P. Novak et al [71] used PBD to study the ion exchange of PPy in different nonaqueous media and found that the kind of ion exchanged (cation or anion) depends on the solvent. While anions are mainly exchanged in ACN, cations are exchanged in PC. The controled release of an anticancer drug (5-fluorouracil) was also demonstrated using PBD [72].

Polythiophene

The technique was used to study the formation of radical cations in poly(3-methylthiophene) [73]. It was also used to study the deposition of poly(thiophene) [74] and poly(alkylterthiophenes) [75].

Polynaphtols

The electropolymerization of 1-naphtol in nonaqueous media produces an electroactive polymer with fused naphtalene and furane rings [76]. The ion exchange of the polymer, studied by PBD, reveals a strong effect of the cation size on the exchange. While anions are exchanged in tetrabutylammonium perchlorate, in LiClO$_4$, the ion

exchange is mainly made by cations. In the latter system, using CVD and chronodeflectometry, a clear kinetic effect is detected. At high scan rates (short time) anions are exchanged while at slow scan rates (long time) cations are exchanged [77].

Polyaniline and related polymers

The CVD and CV responses of a PANI film, in 1 M HCl, is shown in Figure 18. During the first voltammetric oxidation peak, a negative deflection pre peak (proton expulsion) is observed first, followed by a positive deflection peak (anion insertion). In the potential range of the second peak, a negative deflection peak (ion expulsion) is observed. In the reduction scan, the behavior is the opposite [78]. A possible scheme to explain the ion exchange is shown below:
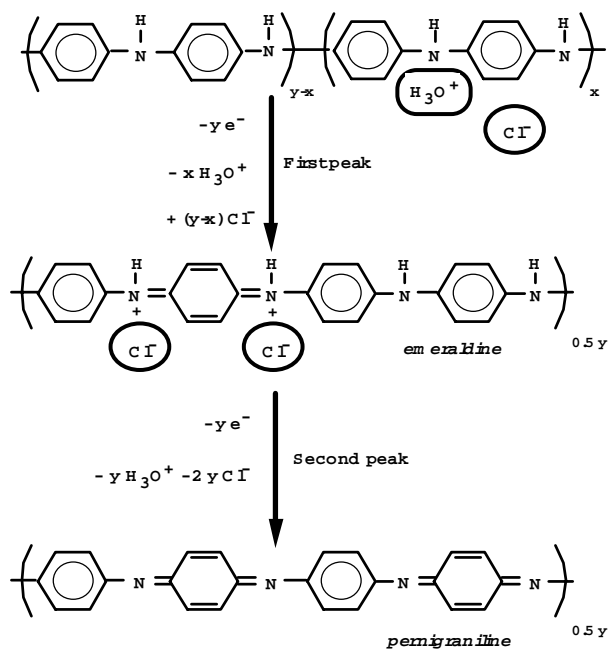
As it can be seen, it is assumed that the reduced state of PANI is protonated. The formation of radical cations is accompanied initially by proton expulsion. When all the available protons are expelled, anions are inserted to maintain charge electroneutrality. If the proton concentration in the solution is increased, more reduced PANI is protonated and the negative deflection signal increases, while the positive signal decreases. The ratio:

$$f_{PBD} = \frac{\theta(-)}{(\theta(-)+\theta(+))} \tag{31}$$

is directly related to the amount of reduced PANI protonated. The plots of f_{PBD} as a function of proton concentration are similar to titration curves. The median value (equivalent to a pKa) depends on the nature of the acid used [79]. During the second oxidation process, the emeraldine salt state is converted into pernigraniline base. The oxidation is accompanied by deprotonation, which accounts for the ion expulsion and the addition of salts also affects the ion exchange mechanism [80]. In nonaqueous media, the

polymer exchange anions during both redox processes [81]. The ion exchange has been studied in other media using PBD [82, 83].

If the polymer is prepared in presence of a polyelectrolyte, like poly(vinylsulfonate), the ion exchange is altered [84]. The polyelectrolyte, retained inside the polymer, compensate the positive charge on oxidation. However, both the protonation equilibria of PANI and the polyelectrolyte have to be taken into account to explain the observed ion fluxes.

Sulfonated polyaniline.

An easy way to alter the ion exchange mechanism implies fixing negative charges to the polymer backbone. The incorporation of sulfonate groups, to produce sulfonated polyaniline, could be effected by electrophilic sulfonation of PANI [85], copolimerization of aniline with aminosulfonic acids [86] or nucleophilic addition [87]. In all cases, the ion exchange is altered. In aqueous media, both redox steps present negative deflection on oxidation [81]. This suggests that both redox processes involve proton expulsion, being the negative charge compensated by the covalently linked anions. In nonaqueous media, both redox process show cations fluxes. This is surprising since the sulfonating degree (50%) is lower than the 100% necessary to compensate for all the positive charge. It seems apparent that solution counterions (ClO_4^-) form ion pairs with sulfonate and lithium, being retained upon polymer reduction. Other data, obtained using EQCM with different anions and cations, confirm the PBD results [81].

Poly(N-methylaniline)

While incorporation of anionic groups should alter the ion exchange mechanism during the first oxidation process, alkylation of the amine nitrogen should block the deprotonation altering the second redox process. Indeed, poly(N-methylaniline) a polymer where each amino nitrogen is blocked shows a CVD with a positive deflection during the second oxidation process, indicating that anions are inserted where two anions and a proton are expelled in PANI [88]. The mechanism:

$$\text{PNMANI} \xrightarrow{-e^- + A^-} \text{PNMANI}^+(A^-) \xrightarrow{-e^- + A^-} \text{PNMANI}^{++}(A^-)_2 \text{ [XVIII]}$$
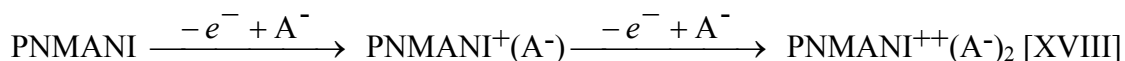
is confirmed by EQCM [88].

Poly(o-toluidine) (POT)

Hillman and coworkers [90-92] have studied the redox coupled ion exchange in POT. Using the convolution method, they could separate the flux of anions and cations in the ion exchange.

1.5 Combination of PBD with other techniques

PBD techniques, like any other electrochemical technique, could profit from its combination with other techniques.
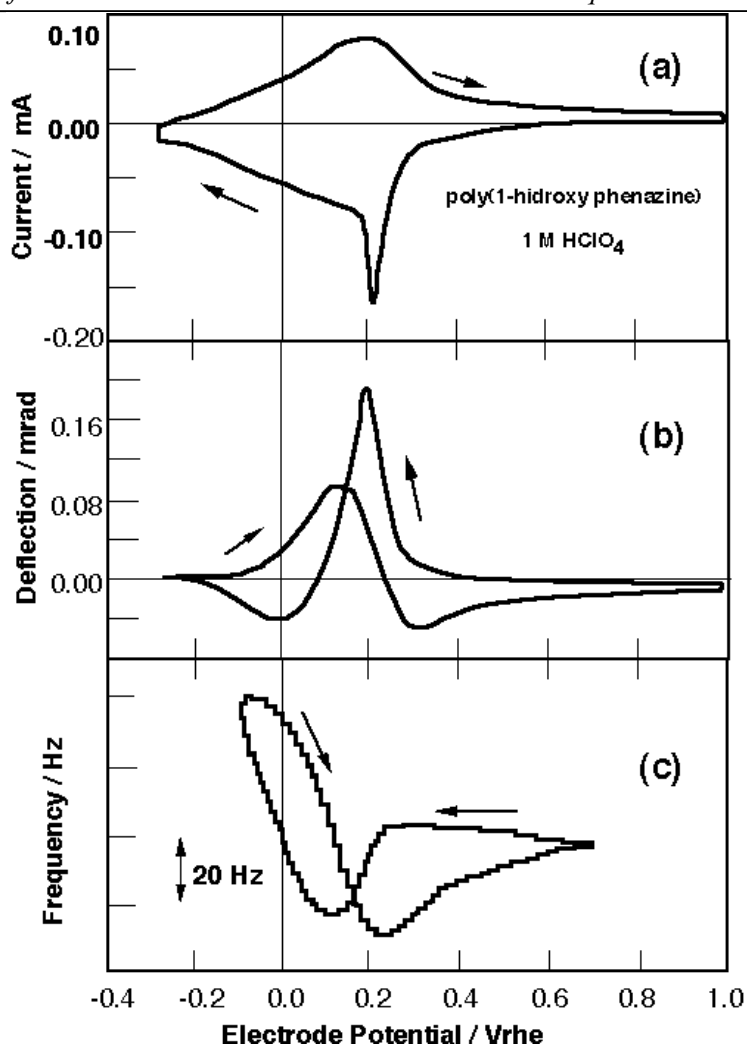
Figure 19: *Combined electrochemical quartz crystal microbalance (EQCM) and Probe Beam Deflection (PBD) study of poly(1-hidroxyphenazine) films.(a) Current, (b) Deflection (PBD) and (c) Frequency (EQCM). v = 50 mV/s. Solution = 1 M HClO₄.*

1.5.1 Combination of PBD with EQCM

In the previous section, it was shown that PBD combined with EQCM helps to clarify the ion exchange of PANI, PNMANI and SPAN. A more complex system, poly(1-hydroxyphenazine) (pOHPh) was also studied [89] (see Figure 19). Both deflection and EQCM agree with a two step mechanism:

$$(pOHPh)H_2 \xrightarrow{\;-e^- + A^-\;} (pOHPh)H_2^+(A^-) \xrightarrow{\;-e^- - A^- - HA\;} pOHPh \quad (XIX)$$
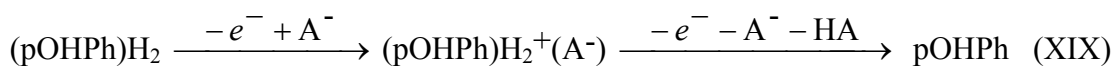
Chronodeflectometric measurements allows to detect kinetic effects during the ion exchange. PBD and EQCM has also been combined by measuring in the same electrode [90]. The study of POT using such approach [91] allows to detect histeresis effects and to

separate the solvent fluxes from ion exchange [92]. Moreover, the use of PBD suggests that protons are indeed exchanged during the first oxidation process of PANI. Therefore it was looked at in aproppiate conditions by EQCM, being able to detect them [93]. Also, the temporal resolution of ion and solvent exchange was achieved in $Ni(OH)_2$/LiOH [94] and $POT/HClO_4$ films [95]. Recently, PBD was combined with electroacoustic EQCM to investigate redox coupled ion exchange in poly(vinylferrocene) [96].

1.5.2 Combination with in-situ Infrared Spectroscopy.

Previously (1.4.3.5), it has been described the use of PBD combined with MIRFTIRS to study poly(1-naphtol). The combined technique was also used to study the ion exchange in poly(5-amino-1-naphtol) [97] and poly(5-amino-1,4-naphtoquinone) [98].

1.5.3 Combination with Photothermal Deflection Spectroscopy.

The experimental set-up for PDS and PBD techniques is very similar, thus it is easy to combine them. This approach was used by Cairns and co-workers to study the oxidation of Cu in basic media [12] and Koetz et al to study the electrochromism of anodic iridium oxide thin films [39].

2 Conclusions

PBD techniques are able to detect ion gradients with have a great sensitivity (down to 2% of a monolayer). They are especially useful to study redox coupled ion exchange in electroactive polymer or oxide films. The difusional delay, present in the experimental data, could be used to determine diffusion coefficients. The technique could be used to study electrodes with different shapes and nature, including porous and sintered materials. The use of high surface area electrodes is advantageous since the signal/noise ratio of those electrodes is improved compared with flat electrodes. The analysis of redox reactions in solution is quite complex. The distortion of the data, due to the diffusional delay, could be overcome by the use of sampling techniques (pulse chronodeflectometry) or data processing schemes (convolution or digital simulation).

Future applications of the PBD techniques could involve the study of: ion fluxes in liquid-liquid interfacial electrodes (ITIES); ion exchange in enzymatic and/or membrane electrodes; and ion fluxes in metal corrosion.

References

[1]   A.J. Bard, L. Faulkner, *Electrochemical Methods*, Wiley, New York, **1984**.
[2]   H.D. Abruña, *Electrochemical Interfaces. Modern Techniques for In-situ Interface Characterization* Ed., VCH, Weinheim, 1991; R.J. Gale, *Spectroelectrochemistry. Theory and Practice*, Ed., Plenum Press, New York, **1988**.
[3]   R.H. Mueller in *Advances in Electrochemistry and Electrochemical Engineering*, Vol 9, J. Wiley & Sons, New York, **1973**.
[4]   G. Horanyi, G. Inzelt, *Electrochim. Acta* **1988**,*33*, 947.
[5]   K. Shimazu, K. Murakoshi, H. Kita, *J. Electroanal. Chem*. **1990**, *277* ,347.

[6]   K. Rajeswahr, R.O. Lezna, N.R. de Tacconi, *Anal. Chem*. **1992**, *64*, 429A; M. Lapkowski, E.M. Genies, *J. Electroanal. Chem*. **1990**, *284*, 127.

[7]   A.J. Bard, G. Denault, C. Lee, D. Mandler, D.O. Wipf, *Acc.Chem.Res*. **1990**, *23*, 357.

[8]   T. Kobayashi, H. Yoneyama, H. Tamura, *J. Electroanal.Chem*. **1984**, *177*, 281.

[9]   R.L. McCreery, *Prog. Analyt. Spectrosc*. **1988**, *11*, 141.

[10]   H.J. Kragt, C.P. Smith, H.S. White, *J. Electroanal. Chem.* **1990**, *378*, 403.

[11]   A.C. Boccara, D. Fournier, J. Badoz, *Appl. Phys. Lett*. **1980**, *36*, 130; A.C. Tam, *Rev. Mod. Phys*. **1986**, *58*, 381.

[12]   R.E. Russo, F.R. McLarnon, J.D. Spear, E.J. Cairns, *J. Electrochem. Soc*. **1987,** *134*, 2783.

[13]   B.S.H. Royce, D. Voss, A. Bocarsly, *J. de Physique* **1983**, *44*, 323; J. Pawliszyn, M.F. Weber, M.J. Dignam, A. Mandelis, R.D. Venter, S-M. Park, *Anal. Chem*. **1986**, *58*, 236; A. Mandelis, B.S.H. Royce, *Appl. Optics* **1984**, *23*, 2892.

[14]   J.D. Rudnicki, F.R. McLarnon, E.J. Cairns in *Techniques for Characterization of Electrodes and Electrochemical Processes*, R. Varma, J.R. Selman,Eds., Plenum, New York, **1991**.

[15]   C. Barbero, M.C. Miras, R. Koetz, *Electrochim. Acta* **1992**, *37*, 429.

[16]   J.D. Rudnicki, G.M. Brisard, H.A. Gasteiger, R.E. Russo, F.R. McLarnon, E.J. Cairns, *J. Electroanal. Chem*. **1993**, *3628*, 55.

[17]   M.A. Vorontyntsev, C. Lopez, E. Vieil, *J. Electroanal. Chem*. **1994**, *368*, 155.

[18]   J.M. Rosolen, M. Fracastoro-Decker, F. Decker, *J. Electroanal.Chem*. **1993**, *346*,119.

[19]   V.M.M. Lobo, *Handbook of Electrolyte Solutions*, Elsevier, Amsterdam, **1989**

[20]   C. Barbero, M.C. Miras, R. Koetz, O. Haas, *Solid State Ionics* **1993**, *60*, 167.

[21]   F. Decker, R.T. Neuenschwander, C.L. Cesar, A.F.S. Penna, *J. Electroanal. Chem*. **1987**, *228*, 483

[22]   Y. Awakura, M. Okada, Y. Kondo, *J. Electrochem. Soc*. **1977**, *124*, 1051 and refs. in the text .

[23]   M:A. Tamor, M. Zanini, *J. Electrochem. Soc*. **1986**, *133*, 1399.

[24]   R. Eriksson, C. Barbero, D. Simonsson, R. Koetz, *Extended Abstracts of The Electrochemical Society Meetings*, New Orleans **1993**, *93-2*, 326.

[25]   M. Fracastoro-Decker,F. Decker, *J.Electroanal. Chem*. **1989,** *266*, 215.

[26]   M. Mathias, *J. Electroanal. Chem.* **1996**, *407*,115.

[27]   J.M. Saveant, D. Tessier, *J. Electroanal. Chem*. **1975**, *65*, 57.

[28]   K.B. Oldham, *Anal. Chem*. **1986**, *58*, 2296

[29]   R.C. Engstrom, R.M. Wightman, E.W. Kristensen, *Anal. Chem*. **1988**, *60*, 652.

[30]   J.C. Myland, K.B. Oldham, *Anal. Chem*. **1999**, *71*, 183.

[31]   J. Pawliszyn, *Anal. Chem*.**1988**, *60*, 1751

[32]   E. Vieil, *J. Electroanal. Chem*. **1996**, *164*, 2296 and refs therein.

[33]   M. J. Henderson, A. R. Hillman, E. Vieil and C. Lopez, *J. Electroanal. Chem*. **1998**, *458*, 241.

[34]   M.J. Henderson, A.R. Hillman, E. Vieil, *Electrochim. Acta* **2000**, *45*, 3185.

[35]   E. Vieil, K. Meerholz, T. Matencio, J. Heinze, *J. Electroanal. Chem*. **1994**, *368*, 183.

[36]   M.A. Vorontyntsev, C. Lopez, E. Vieil, *J. Electroanal. Chem*. **1994**, *368*, 155.

[37]   E. Vieil, C. Lopez, *J. Electroanal. Chem*. **1999**, *466*, 218.

[38]   R. Kötz, C. Barbero, O. Haas*, J. Electroanal. Chem*. **1990**, *296*, 37.

[39]   R. Koetz, C. Barbero, O. Haas, *Ber. Bunsenges. Phys. Chem*. **1993**, *97*, 427.

[40]   G. Inzelt, V. Kertész, G. Lang, *J. Phys. Chem*. **1999**, *73*, 6104 and refs in the text.

[41]   V. Kertész, G. Inzelt, C, barbero, R. Koetz, O. Haas, *J. Electroanal. Chem*. **1995**, *392*, 91.

[42]   D. Dini, S. Cattarin, F. Decker, *J. Electroanal. Chem*. **1998**, *446*, 7.

[43]   R.E. Russo, F.R. McLarnon, J.D. Spear, E.J. Cairns, *J. Electrochem. Soc*. **1987,** *134*, 2783; G. M. Brisard, J. D. Rudnicki, F. McLarnon and E. J. Cairns, *Electrochim. Acta* **1999**, *40*, 859.

[44]   R. Eriksson, *Electrochim. Acta* **1996**, *41*, 871.

[45]   L.M. Abrantes, M.C. Oliveira, E. Vieil *Electrochim. Acta*, **1996**, *41*, 1515.

[46]   J-N Han and S-I Pyun, *Electrochim. Acta* **2000,** *45*, 2781

[47]   S.Cattarin, E. Pantano and F. Decker, *Electrochem. Comm*. **1999**, *1*, 483

[48]   S. Cattarin, F. Decker, D.Dini, *J. Phys. Chem. B*. **1998**, *102*; 4779.

[49]   E.D. Bidoia, F. McLarnon, E.J. Cairns, *J. Electroanal. Chem*. **2000**, *482*, 75.

[50]   M.D. Levi, E. Levi, Y. Gofer, D. Aurbach, E. Vieil, J. Serose, *J. Phys. Chem*. **1999**, *103*, 1499.

[51]   C.W. Liu, S.J. Cheng, G.J. Cheng, D.Y. Sun, *J. Electrochem. Soc*. **1996**, *143*, 3787**.**

[52]   B.E. Conway, *Electrochemical Supercpacitors. Scientific Fundamentals and technological applications,* New York, Kluwer Academic Publishers, **1999**.

[53]   G.A. Planes, M.C. Miras, C. Barbero, in *Advanced Batteries and Supercapacitors,* PV-2001, The Electrochemical Society, Pennigton, **2002**.

[54]   M. Bardin, P. Loheac, M.A. Petit, V, Plichon, N. Richard, *New J. Chem*. **1995**, *19*, 59

[55]   J.M. Rosolen, F. Decker, M. Fracastoro-Decker, A. Gorenstein, R.M. Torresi, S.I. Córdoba de Torresi, *J. Electroanal. Chem*. **1993**, *354*, 273.

[56]   H.M. French, M.J. Henderson, A. R. Hillman, E. Vieil, *J. Electroanal. Chem*. **2000**, *500*, 192

[57]   C. Barbero, G.A. Planes, M.C. Miras, *Electrochem. Commun*. **2001**, *3*, 113.

[58]   A. Barbu, V. Plichon, *Eletrochim. Acta* **1997**, *42*, 489.

[59]   V. Plichon, S. Besbes, *J. Electroanal. Chem*. **1990**, *284*, 141

[60]   C.W. Liu, Y. Wang, G.Y. Zhu, S.J. Dong, *Electrochim. Acta* **1997**, *42*, 1795.

[61]   E. Csahok, E. Viel, G. Inzelt, *J. Electroanal. Chem*. **1998**, *457*, 251.

[62]   V. Plichon, E. Even, G. Benier, *J. Elrectroanal. Chem*.**1991**, *305*, 195.

[63]   A. Merle, E. Maurin, J.P. Morand, *J. Chem. Phys*. **1989**, *86*, 173.

[64]   O. Haas, *Faraday Discuss. Chem. Soc*. **1988**, *88*,123; O. Haas, J. Rudnicki, F.R. McLarnon, E.J. Cairns, *J. Chem. Soc. Faraday Trans*. **1991**, *87*, 939.

[65]   C. Barbero, E.J. Calvo, M.C. Miras, R. Koetz, O. Haas, *Langmuir* **2002**, *18*, 2756.

[66]   V.M. Schmidt, C. Barbero, R. Koetz, *J. Electroanal. Chem*. **1993**, *352*, 301

[67]   C. Lopez, M.F. Mendes Viegas, G. Bidan, E. Vieil, *Synth. Met*. **1994**, *63*, 73

[68]   T. Matencio, M.-A. De Paoli, R.C.D. Peres, R.M. Torresi, S.I. Córdoba de Torresi, *Synth. Met*. **1995**, *71*, 59.

[69]   G. Bidan, C. Lopez, F. Mendes-Viegas and E. Vieil, A. Gadelle, *Biosensors and Bioelectronics* **1995**, *10*, 219.

[70]   M. A. Petit, V. Plichon and C. Colin, *Electrochim. Acta* **2000**, *45*, 1953

[71]   P.Novak, R. Koetz, O. Haas, *J. Electrochem. Soc.* **1993**, *140*, 37.

[72]   H. Huang, C. Liu, B. Liu, G. Cheng and S. Dong, *Electrochim. Acta* **1998**, *43*, 999.

[73]   A. Merle, E. Maurin, J.P. Morand, *J. Chem. Phys.* 1989, *86*, 173.

[74]   L.M. Abrantes, J.P. Correia, J. González, *J. Chim. Phys.-Chim. Biol.* **1998**, *95*, 1172.

[75]   D. Dini, F. Decker and G. Zotti, *Synth. Metals* **1999**, *101*, 22.

[76]   M.C. Pham, J. Moslih, P.C. Lacaze, *J. Electroanal. Chem.* **1990**, *278*, 415.

[77]   M-C. Pham, J. Moslih, C. Barbero, O. Haas, *J. Electroanal. Chem.* **1991**, *316*, 143.

[78]   C. Barbero, M.C. Miras, O. Haas and R. Kötz, *Synth. Met.* **1993**, *55*, 1539.

[79]   C. Barbero, M.C. Miras, O. Haas, R. Kötz, *J. Electrochem. Soc.* **1991,** *138*, 669.

[80]   C. Barbero, R. Koetz, M. Kalaji, L. Nyholm, L.M. Peter. *Synth. Met.* **1993,** *55-57*, 1545.

[81]   C. Barbero, M.C. Miras, R. Kötz, *J. Electroanal. Chem.* **1997,** *437*,191.

[82]   T. Matencio, E. Vieil, *Synth. Met.* **1991**, *44*, 349.

[83]   K. Koziel, M. Lapkowski, E. Vieil, *Synth. Met.* **1997**, *84*, 91.

[84]   C. Barbero, M.C. Miras, R. Koetz, O. Haas, *J. Electrochem. Soc.* **1997**, *144*, 4170.

[85]   C. Barbero, M.C. Miras, B. Schnyder, O. Haas, R. Koetz, *J. Mater. Chem.* **1994**, *4*, 1775 and refs in the text.

[86]   C. Barbero, R. Koetz, *Adv. Mater.* **1994**, *6*, 577.

[87]   H. Salavagione, G.M. Morales, M.C. Miras, C. Barbero, *Acta Polym.* **1999**, *50*, 40.

[88]   C. Barbero, M.C. Miras, R. Koetz, O. Haas, *J. Electroanal. Chem.* **1991**, *310*, 437.

[89]   M.C. Miras, C. Barbero, R. Koetz, O. Haas, V.M. Schmidt, *J. Electroanal. Chem.* **1992**, *338*, 279

[90]   M.J. Henderson, A.R. Hillman, E. Vieil, *J. Electroanal. Chem.* **1998**, *454*, 1

[91]   M.J. Henderson, A.R. Hillman, E. Vieil, C. Lopez, *J. Electroanal. Chem.* **1998**, *458*, 241

[92]   M.J. Henderson, A.R. Hillman, E. Vieil, *J. Phys. Chem. B.* **1999**, *103*, 8899.

[93]   M.C. Miras, C. Barbero, R. Kötz and O. Haas, *J. Electroanal. Chem.* **1994,** *369*, 203.

[94]   H. M. French, M. J. Henderson, A. R. Hillman, E. Vieil, *Solid State Ionics* **2002,** *150*, 27

[95]   M. J. Henderson, A. R. Hillman, E. Vieil, *Electrochim. Acta* **2000,** *45*, 3885

[96]   C. Barbero, E.J. Calvo, R. Etchenique, G.M. Morales, M. Otero, *Electrochim. Acta* **2000,** *45*, 3895.

[97]   C. Barbero, O. Haas, M. Mostefai, M-C. Pham, *J. Electrochem. Soc.* **1995,** *142*, 1829.

[98]   B. Piro, E.A. Bazzaoui, M-C. Pham, P. Novak, O.Haas, *Electrochim.Acta*. **1999**, *44*, 1953.

[99]   *CRC Handbook of Chemistry and Physics*, 68 Ed., CRC Press, **1978,** New York.

[100] R.N. O'Brien in *Physical Methods of Chemistry*, A. Weissberger, B.W. Rossiter, Eds., Wiley Interscience, New York, **1972**.

APPENDIX

Table 2: *Variation of refractive index with concentration for common ions*.*

Species	$\partial n / \partial C$ x 10^3	Species	$\partial n / \partial C$ x 10^3	Species	$\partial n / \partial C$ x 10^3
CH_3COOH	39.9	H_3PO_4	8.35	O_2	-14.4[b]
$HONH_4$	0.91	$KHCO_3$	9.78	H_2	-12.8[b]
$ClNH_4$	9.47	$KHC_8H_4O_4$	37.64	NaH_2PO_2	22.1[c]
$(NH_4)_2SO_4$	18.54	KBr	13.71	Na_2HPO_3	10.7[c]
$BaCl_2\ 2H_2O$	28.35	$K_2CO_3\ 1.5H_2O$	21.56	$LiClO_4$	6.69[d]
$CaCl_2\ 2\ H_2O$	23.96	KCl	9.6	$NaCl$	9.55
$CsCl$	12.47	K_2CrO_4	38.37	$NaClO_4$	7.36
$CoCl_2\ 6H_2O$	26.58	$K_2Cr_2O_7$	51.86	$HClO_4$	6.8[d]
$CuSO_4\ 5H_2O$	26.33	$K_3Fe(CN)_6$	51.64	$NaOH$	9.76
$FeCl_3\ 5H_2O$	41.14	$K_4Fe(CN)_6\ 3H_2O$	70.55	$NaHCO_3$	10.48
$HCOOH$	2.52	KOH	10.07	$Na_2CO_3\ 10H_2O$	21.25
HCl	7.94	KI	21.05	$NaCr_2O_7\ 2H_2O$	50.4
$Pb(NO_3)_2$	36.43	KNO_3	8.98	$Na_4Fe(CN)_6$	71.74
$LiCl$	8.36	$K_2C_2O_4\ H_2O$	20.96	Na_2MoO_4	34.06
$MgCl_2\ 6H_2O$	20.4	KH_2PO_4	14.15	$NaNO_3$	8.64
$MgSO_4.\ 7H_2O$	20.8	$KHPO_4\ 3H_2O$	24.95	$Na_3PO_4\ 12H_2O$	37.48
$MnSO_4\ H_2O$	23.7	K_2SO_4	19.51	$Na_2HPO_4\ 7H_2O$	25.01
$NiSO_4\ 6H_2O$	29.21	$KSCN$	17.3	$NaH_2PO_4\ H_2O$	14.4
HNO_3	7.8	$AgNO_3$	17.28	$Na_2SO_4\ 10H_2O$	19.24
$Na_2S_2O_3\ 5H_2O$	29.69	Na thartrate	30.35	$NaBr$	13.56
CCl_3COOH	19.5	$ZnSO_4$	25.55	$SrCl_2\ 6H_2O$	27.09
H_2O_2	1.4[a]	CH_3COONa	10.63	H_2SO_4	11.05

* The values are valid for concentrations below 2 M and were obtained by graphing the data in the literature [99] unless otherwise stated in the Table. [a]Ref 38; [b]Ref [100]; [c]Ref. 49; [d]Ref. 17.

Symbols and acronyms

PDS	Photothermal Deflection Spectroscopy
PBD	Probe Beam Deflection
EQCM	Electrochemical Quartz Crystal Microbalance
PSCD	Potential Step Chronodeflectometry
CSCD	Current Step Chronodeflectometry
ACD	Alternate Current Deflectometry
CVD	Cyclic VoltaDeflectometry
NPVD	Normal Pulse VoltaDeflectometry
DPVD	Differential Pulse VoltaDeflectometry
q	deflection angle (radians)
n	refractive index
l	interaction pathlenght between the probe beam and the sample
C	Molar concentration of solution species
T	Temperature of the solution(^{o}C)
x	distance from probe beam to the surface of the sample (mm)
t	time (s)
$\partial n / \partial C$	Variation of refractive index with concentration (mol^{-1})
l	wavelength (nm)
w	frequency (Hz)
t_{max}	time to reach the deflection maximum value
i	current (A)
j	current density (A/cm^2)
n_e	number of electrons exchanged
F	Faraday constant
A	area (cm^2)
D	Diffusion coefficient (cm^2/s)
tf	Transference number of the ion
Q	Electrochemical charge (coulombs)
U	Temporal constant in NPVD and DPVD
H_{ion}	Capacity of ion exchange
C_{ele}	Electrical capacitance (farads)
C_{ion}	Concentration of exchanged ions at x=0
z_i	Charge of species i
J_i	Flux of species i
$H(x,t)$	Transference function for planar semi-infinite diffusion
G	Surface concentration of redox centres (mol cm^{-2})
ACN	Acetonitrile
PC	Propylene carbonate
PANI	Polyaniline
SPAN	Sulfonated polyaniline
PVF	poly(vinylferrocene)

AIROF	Anodic Iridium Oxide Film
pOHPh	poly(1-hydroxiphenazine)
PPy	polypirrole
PNMANI	poly(N-methylaniline)
PVS	poly(vinylsulfonato)
PT	poly(thiophene)
TsO$^-$	toluensulfonate ion
SDS	Sodium Dodecilsulfate
SCE	Saturated Calomel Electrode
NHE	Normal Hydrogen Electrode
UPD	Under Potential Deposition
MIRFTIRS	Multiple Internal Reflection Fourier Transform Infrared Spectroscopy